NASA CONTRACTOR REPORT

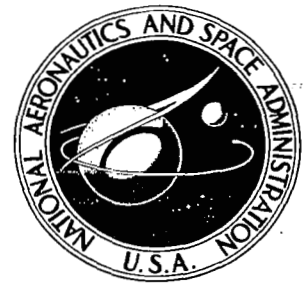

NASA CR-2663

A STUDY OF TURBULENT FLOW BETWEEN PARALLEL PLATES BY A STATISTICAL METHOD

R. Srinivasan, D. P. Giddens, L. H. Bangert, and J. C. Wu

Prepared by
GEORGIA INSTITUTE OF TECHNOLOGY
Atlanta, Ga. 30332
for Langley Research Center

NATIONAL AERONAUTICS AND SPACE ADMINISTRATION • WASHINGTON, D. C. • APRIL 1976

1. Report No.	2. Government Accession No.	3. Recipient's Catalog No.
NASA CR-2663		

4. Title and Subtitle	5. Report Date
A STUDY OF TURBULENT FLOW BETWEEN PARALLEL PLATES BY A STATISTICAL METHOD	April 1976
	6. Performing Organization Code

7. Author(s)	8. Performing Organization Report No.
R. Srinivasan, D. P. Giddens, L. H. Bangert & J. C. Wu	
	10. Work Unit No.

9. Performing Organization Name and Address	11. Contract or Grant No.
Georgia Institute of Technology Atlanta, Georgia 30332	NGR11-002-157 NGR11-002-159
	13. Type of Report and Period Covered
12. Sponsoring Agency Name and Address	Contractor Report
National Aeronautics & Space Administration Washington, DC 20546	14. Sponsoring Agency Code

15. Supplementary Notes

Langley Technical Monitor: John S. Evans, Jr.

Final Report

16. Abstract

Turbulent Couette flow between parallel plates is studied from a statistical mechanics approach utilizing a model equation, similar to the Boltzmann equation of kinetic theory, which was proposed by Lundgren from the velocity distribution of fluid elements. Solutions to this equation are obtained numerically, employing the discrete ordinate method and finite differences. Two types of boundary conditions on the distribution function are considered, and the results of the calculations are compared to availabe experimental data. The research establishes that Lundgren's equation provides a very good description of turbulence for the flow situation considered and that it offers an analytical tool for further study of more complex turbulent flows. The present work also indicates that modelling of the boundary conditions is an area where further study is required.

17. Key Words (Suggested by Author(s))	18. Distribution Statement
Turbulent Couette flow Statistical mechanics Discrete ordinate method Probability distribution function	Unclassified - Unlimited Subject Category 34

19. Security Classif. (of this report)	20. Security Classif. (of this page)	21. No. of Pages	22. Price*
Unclassified	Unclassified	57	$4.25

For sale by the National Technical Information Service, Springfield, Virginia 22161

TABLE OF CONTENTS

LIST OF SYMBOLS

B	Constant used in equation for law of the wall, (5.0)
$\vec{c}$	Turbulence velocity
c_1, c_2	Constants used in equation for dissipation rate
$\overline{-c_x c_y}$	Reynolds stress per unit mass
$\overline{c_y^2}$	Mean square of y-component of turbulence velocity
$2d$	Distance between plates in Couette flow
f	Distribution function of velocities of fluid element
F	Gaussian (equilibrium) distribution function
g, j, h, j_v	Reduced distribution functions
G, J, H, J_v	Reduced equilibrium distribution functions
K	Constant of proportionality in expression for relaxation time
p	Pressure
P_K	Non-dimensional pressure gradient
Q_y	Flux of turbulence kinetic energy
$\vec{r}$	Position vector
Re	Reynolds number based on plate velocity in Couette flow, $(u_w\, d/\nu)$
Re_*	Reynolds number based on friction velocity, $(u_*\, d/\nu)$
u_*	Friction velocity, $(\tau_w/\rho)^{\frac{1}{2}}$
u_w	Plate velocity for Couette flow
$3U^2$	Mean square of velocity fluctuations
$\vec{u}$	Time averaged flow velocity
$\vec{v}$	Instantaneous velocity of fluid element
x, y	Cartesian coordinates parallel and perpendicular to primary flow direction

y_*	$u_* y/\nu$
ϵ	Viscous dissipation rate per unit mass
κ	von Karman constant, (0.41)
ν	Kinematic viscosity
ν_T	Turbulent diffusivity
ρ	Fluid density
σ_ϵ	Prandtl-Schmidt number for ϵ
τ	Relaxation time
τ_w	Wall shear stress

Superscripts

$(\bar{})$	Time averaged quantities
$(\hat{})$	Non-dimensionalized quantities

Subscripts

i	Evaluated at the physical node i
σ	Evaluated at the discrete velocity point c_σ
x	x component
y	y component
B	Quantities denoting boundary conditions

A STUDY OF TURBULENT FLOW BETWEEN PARALLEL PLATES BY A STATISTICAL METHOD

by

R. Srinivasan, D. P. Giddens, L. H. Bangert and J. C. Wu
School of Aerospace Engineering
Georgia Institute of Technology

INTRODUCTION

Similarities between the statistical behavior of molecules in a gas and the velocity fluctuations of fluid elements in a turbulent flow suggest the possibility of describing both phenomena in terms of a velocity distribution function from which mean properties may be computed by taking appropriate moments. The literature abounds with efforts to exploit this analogy between the two areas of the field of statistical mechanics. From another point of view, there are potential simplifications in modeling turbulence behavior at the level of the velocity distribution function (or, the probability density), rather than modeling individual correlations. Of particular interest are two recent studies which have attempted to develop theoretical treatments for practical application[1,2]. Lundgren[1] begins with the incompressible Navier-Stokes equations in a form which assumes either an infinite fluid region or a constant pressure boundary condition. A hierarchy of equations for multipoint distribution functions is developed which strongly resembles the Bogoliubov-Born-Green-Kirkwood-Yvon[3] (BBGKY) equations. In a subsequent work Lundgren[4] attempts to close the system at the one-point level by employing a relaxation model identical in form to the Bhatnager-Gross-Krook (BGK) model of kinetic theory. This model equation is not, within itself, sufficient to define a turbulent flow. An additional equation is required to relate the turbulence dissipation rate to other flow properties. This, in effect, implies that an ad hoc assumption must be made regarding the relaxation rate in the model. Lundgren applies his equations to several idealized problems in which no solid boundaries are present.

Chung[2,6] has taken a very different approach but arrived at a similar governing equation for the distribution function. His analysis was developed from ideas of generalized Brownian motion and resulted in a modified

Fokker-Planck equation. The analysis has been extended to account for chemical species and reactions[7]. Chung likewise finds it necessary to make ad hoc assumptions on mixing length if his equations are to be self-contained. The resulting model is applied to the problem of plane Couette flow of an incompressible, single-species gas by employing moment methods familiar in kinetic theory[8]. In these methods specific functional forms are assumed for the distribution function and unknown coefficients are found in the solution.

The present work describes the solution of Lundgren's model equation for plane Couette flow. This provides an important extension of his previous studies in that the flow field is bounded by solid surfaces and in that it represents a flow for which experimental data are available. The solution is accomplished by an extension of the discrete ordinate method[9,10] as developed for problems in rarefied gasdynamics. This differs from the moment method selected by Chung in that no a priori assumption is enforced upon the form of the distribution function. Results obtained in the present study are compared with Chung's work and with available experimental data.

Perhaps an interesting analogy between the application of the discrete ordinate method and the moment method is that of the improvement provided in turbulent boundary layer calculations by the use of numerical solution to the partial differential equations themselves as opposed to the classical integral method used earlier. A finer detail of flow structure is afforded by the direct numerical solution.

GOVERNING EQUATIONS

General Equation for the Distribution Function

The starting point for the present analysis is the lowest order equation for the turbulent distribution function (Eqs. (1) and (2), Ref. 4)

$$\frac{\partial f}{\partial t} + \vec{v} \cdot \frac{\partial f}{\partial \vec{r}} + \left(- \frac{1}{\rho} \frac{\partial \bar{p}}{\partial \vec{r}} + \nu \frac{\partial}{\partial \vec{r}} \cdot \frac{\partial}{\partial \vec{r}} \vec{u} \right) \cdot \frac{\partial f}{\partial \vec{v}} \tag{1}$$

$$= - \frac{1}{\tau} \left(f - F \right) + \frac{1}{3} \frac{\epsilon}{U^2} \frac{\partial}{\partial \vec{v}} \cdot \left(\vec{v} - \vec{u} \right) f$$

where $f(\vec{r}, \vec{v}, t)\, d\vec{v}$ is the probability that the velocity at point $\vec{r}$ in physical space is in the range $\vec{v}$ to $\vec{v} + d\vec{v}$ in velocity space. Pressure, density and kinematic viscosity are symbolized by $\bar{p}$, ρ and ν, respectively. The relaxation time is denoted by τ, which is related to the characteristic turbulence diffusion time. F is a Gaussian (equilibrium) distribution given by

$$F = \left(2\pi U^2 \right)^{-3/2} \exp \left[- (\vec{v} - \vec{u})^2 / 2U^2 \right] \tag{2}$$

The time average flow velocity is $\vec{u}$ and $3U^2$ is the mean square of the velocity fluctuations. These are defined as appropriate moments of f. That is,

$$\vec{u} = \int \vec{v}\, f d^3 v$$

$$3U^2 = \int (v - u)^2\, f d^3 v$$

where the integrations are taken over the entire velocity space ($- \infty$ to $+ \infty$ for each component).

Lundgren assumes that the relaxation time is approximately L/U, where L is the integral scale of turbulence, and models this by the equation

$$\frac{1}{\tau} = \frac{K(\epsilon + \frac{3}{2} DU^2/Dt)}{U^2} \tag{3}$$

Here, ϵ is the turbulence dissipation rate, D/Dt is the usual substantial derivative, and K is taken to be a constant whose value is approximately 5.

If the turbulence velocity $\vec{c} = \vec{v} - \vec{u}$ is introduced as an independent variable, the analysis is made somewhat simpler. Making this change of variable and simplifying the physical coordinates to the case of one dimension in anticipation of the application to Couette flow, one obtains

$$c_y \frac{\partial f}{\partial y} - \left(c_y \frac{du_x}{dy} + \frac{1}{\rho} \frac{d\bar{p}}{dx} - \nu \frac{d^2 u_x}{dy^2} \right) \frac{\partial f}{\partial c_x} \tag{4}$$

$$= \frac{1}{\tau} (F - f) + \frac{\epsilon}{3U^2} \left(3f + c_x \frac{\partial f}{\partial c_x} + c_y \frac{\partial f}{\partial c_y} + c_z \frac{\partial f}{\partial c_z} \right)$$

Here, y is taken to be normal to the mean flow and c_x, c_y, c_z are the turbulence velocity components.

Reduced Distribution Functions

A reduction in computer storage requirements is afforded by defining reduced distribution functions according to the following scheme:

$$g(y, c_y) = \int_{-\infty}^{\infty} \int f(y, c_x, c_y, c_z) \, dc_x \, dc_z \tag{5a}$$

$$j(y, c_y) = \int_{-\infty}^{\infty} \int c_x f(y, c_x, c_y, c_z) \, dc_x \, dc_z \tag{5b}$$

$$h\left(y,\ c_y\right) = \int_{-\infty}^{\infty} \int \left(c_x^2 + c_z^2\right) f\left(y,\ c_x,\ c_y,\ c_z\right)\, dc_x\, dc_z \tag{5c}$$

Also, let

$$j_v\left(y,\ v_y\right) = \int_{-\infty}^{\infty} \int \left(c_x + u_x\right) f\left(y,\ c_x,\ c_y,\ c_z\right)\, dc_x\, dc_z \tag{5d}$$

The reduced equilibrium distribution functions, G, J, H and J_v are defined as shown above with f = F. Equation (4) may now be transformed into a system of equations which, although similar in form to the equation for f , are much easier to treat numerically. These become

$$c_y \frac{\partial g}{\partial y} = \frac{1}{\tau}\left(G - g\right) + \frac{\epsilon}{3U^2}\left(g + c_y \frac{\partial g}{\partial c_y}\right) \tag{6a}$$

$$c_y \frac{\partial j}{\partial y} = \frac{1}{\tau}\left(J - j\right) + \left(\nu \frac{d^2 u_x}{dy^2} - \frac{1}{\rho}\frac{d\bar{p}}{dx} - c_y \frac{du_x}{dy}\right) g \tag{6b}$$

$$+ \frac{\epsilon}{3U^2} c_y \frac{\partial j}{\partial c_y}$$

$$c_y \frac{\partial h}{\partial y} = \frac{1}{\tau}\left(H - h\right) + 2\left(\nu \frac{d^2 u_x}{dy^2} - \frac{1}{\rho}\frac{d\bar{p}}{dx} - c_y \frac{du_x}{dy}\right) j \tag{6c}$$

$$+ \frac{\epsilon}{3U^2}\left(-h + c_y \frac{\partial h}{\partial c_y}\right)$$

and

$$v_y \frac{\partial j_v}{\partial y} = \frac{1}{\tau}\left(J_v - j_v\right) + \frac{\epsilon}{3U^2}\left(u_x g + v_y \frac{\partial j_v}{\partial v_y}\right) \tag{6d}$$

$$+ \left(\nu \frac{d^2 u_x}{dy^2} - \frac{1}{\rho}\frac{d\bar{p}}{dx}\right) g$$

These distribution functions should satisfy the constraints

$$\int_{-\infty}^{\infty} g \, dc_y = 1 \tag{7a}$$

and

$$\int_{-\infty}^{\infty} j \, dc_y = \overline{c_x} = 0 \tag{7b}$$

The first of these states that the probability of finding a fluid element somewhere in $\vec{r}$, $\vec{v}$ space is unity, while the second requires that the mean of the longitudinal fluctuating velocity component should be zero.

Moments of Interest

Once the equations are solved for the distribution functions, moments of interest may then be calculated. For example, one obtains

$$u_x = \int_{-\infty}^{\infty} j_v \, dc_y \tag{8a}$$

$$3U^2 = \int_{-\infty}^{\infty} h \, dc_y + \int_{-\infty}^{\infty} c_y^2 \, g \, dc_y \tag{8b}$$

$$\overline{c_x c_y} = \int_{-\infty}^{\infty} c_y \, j \, dc_y \tag{8c}$$

$$\overline{c_y^2} = \int_{-\infty}^{\infty} c_y^2 \, g \, dc_y \tag{8d}$$

$$Q_y = \tfrac{1}{2} \int_{-\infty}^{\infty} c_y h \, dc_y + \tfrac{1}{2} \int_{-\infty}^{\infty} c_y^3 \, g \, dc_y \tag{8e}$$

These are the mean velocity, turbulence kinetic energy, Reynolds stress, mean square of y-velocity component fluctuation, and kinetic energy flux, respectively.

Final Reduced Equations

It is convenient to define the following nondimensional variables:

$$\hat{c}_y = \frac{c_y}{u_*} \quad ; \quad \hat{v}_y = \frac{v_y}{u_*} \quad ; \quad \hat{U} = \frac{U}{u_*} \quad ;$$

$$\hat{u} = \frac{u_x}{u_*} \quad ; \quad \hat{\tau} = \frac{u_* \tau}{d} \quad ; \quad \overline{\hat{c}_x \hat{c}_y} = \hat{p}_{xy} = \frac{p_{xy}}{u_*^2} \quad ; \quad \hat{f} = u_*^3 f \quad ;$$

$$\hat{g} = u_* g \quad ; \quad \hat{h} = \frac{h}{u_*} \quad ; \quad \hat{j} = j \quad ; \quad \hat{j}_v = j_v \quad ; \quad \hat{Q}_y = \frac{Q_y}{u_*^3} \quad ;$$

$$\epsilon = \epsilon d / u_*^3 \quad ; \quad \hat{y} = y/d$$

$$\mathrm{Re}_* = \frac{u_* d}{\nu} \quad ; \quad \hat{P}_k = \frac{d}{\rho u_*^2} \frac{d\bar{p}}{dx}$$

where $2d$ is the distance between the plates, p_{xy} is the turbulence shear stress, ν is the kinematic viscosity, ρ is the density, and $u_* = \left[(p_{xy})_w / \rho \right]^{\frac{1}{2}}$ is the usual friction velocity.

Using these quantities and dropping the superscript " ^ " , for simplicity, the set of governing equations becomes

$$c_y \frac{\partial g}{\partial y} = \frac{1}{\tau}\left(G - g\right) + \frac{\epsilon}{3U^2}\left(g + c_y \frac{\partial g}{\partial c_y}\right) \tag{9a}$$

$$c_y \frac{\partial j}{\partial y} = \frac{1}{\tau}\left(J - j\right) + \left(\frac{1}{Re_*}\frac{d^2u}{dy^2} - P_k - c_y \frac{du}{dy}\right) g \tag{9b}$$

$$+ \frac{\epsilon}{3U^2} c_y \frac{\partial j}{\partial c_y}$$

$$c_y \frac{\partial h}{\partial y} = \frac{1}{\tau}\left(H - h\right) + 2\left(\frac{1}{Re_*}\frac{d^2u}{dy^2} - P_k - c_y \frac{du}{dy}\right) j \tag{9c}$$

$$+ \frac{\epsilon}{3U^2}\left(c_y \frac{\partial h}{\partial c_y} - h\right)$$

and

$$v_y \frac{\partial j_v}{\partial y} = \frac{1}{\tau}\left(J_v - j_v\right) + \frac{\epsilon}{3U^2}\left(u\, g + v_y \frac{\partial j_v}{\partial v_y}\right) \tag{9d}$$

$$+ \left(\frac{1}{Re_*}\frac{d^2u}{dy^2} - P_k\right) g$$

where

$$\frac{1}{\tau} = \frac{K\epsilon}{U^2}$$

It is this set of equations which is to be solved by the discrete ordinate method, subject to the boundary conditions to be discussed subsequently.

Examination of this system of equations reveals that it is not yet completely self-contained. The dissipation rate ϵ is not given as a moment of the distribution function. Therefore, a separate equation for ϵ is required to close the set. Among the possibilities for such an equation for the present problem are the use of an algebraic relationship resulting from setting turbulence production equal to dissipation

$$\epsilon = \frac{u_*^3}{\kappa y} \quad \text{or} \quad \epsilon = 0.7968\ U^3/y \tag{9e}$$

or by use of a differential equation to model ϵ, such as the one derived by Jones and Launder[11] based upon a semi-empirical approach. For Couette flow it is

$$\frac{\nu_T}{\sigma_\epsilon}\frac{d^2\epsilon}{dy^2} + \frac{1}{\sigma_\epsilon}\left(\frac{d\nu_T}{dy}\right)\left(\frac{d\epsilon}{dy}\right) + \frac{2}{3}\ c_1\ \frac{\nu_T}{U^2}\left(\frac{du}{dy}\right)^2\epsilon \tag{9f}$$

$$- \frac{2}{3}\ c_2\ \mathrm{Re}_*\ \frac{\epsilon^2}{U^2} = 0$$

Here, σ_ϵ, c_1 and c_2 are constants and $\nu_T = \mathrm{Re}_*\left(\overline{c_x c_y}\right)/\left(du/dy\right)$. Each of these equations for ϵ has been employed in the present study, and results will be discussed in a subsequent chapter.

BOUNDARY CONDITIONS

One of the difficult aspects of this research is specification of the appropriate boundary conditions. This difficulty arises as a consequence of two factors. First, since the mean velocity is a moment of the distribution function, information from continuum flow only gives the no-slip condition that

$$\vec{u} = \int \vec{v}\, f\, d^3v = 0 \ .$$

Because many functions for f could be specified which satisfy this integral constraint, there is a lack of uniqueness in prescribing f. If f is prescribed as a Dirac delta function which also implies zero instantaneous velocity at the wall, it is difficult to incorporate numerically.

Second, the relaxation time, τ , is difficult to model in the viscous sublayer because of the unknown variation of ϵ and U. Furthermore, in the derivation of the turbulence model equation, the effects due to the presence of the wall were not modeled separately. As a consequence, the validity of the model equation is suspected very near the wall even if a successful relaxation model is obtained. Thus, there is a hesitation in applying the analysis in this zone.

With these considerations in mind there are clearly two fundamental questions to be addressed in the research.

(i) where should the boundary condition on the distribution function be applied, and

(ii) what functional form should it take?

Thus, the present study can actually be divided into two segments: first, to develop the capability of obtaining convergent, stable numerical solutions to the model equation; and second, to examine the validity of various boundary conditions in light of comparison with experimental data [12,13]. This division of the problem virtually parallels the situation arising in calculations of rarefied flows from the Boltzmann equation. In this field the study of gas-surface interactions-- which are used for boundary conditions in solution of the governing equation -- has become almost a separate field of study within itself. Such

could well be the case with the statistical approach to turbulent flows.

Matching to Law of Wall

The course taken in the present work was to confine the application of the turbulent model equation to regions outside the viscous sublayer. Values of $y_* = yu_*/\nu$ from 50 to 100 were selected as the boundary points for the governing equation, and the usual functional forms for law of the wall were assumed to relate the boundary point to wall conditions. This necessitates that certain matching of the numerical solution to law of wall variation at the boundary point be performed. The specific conditions applied are dependent upon the form selected for the distribution function at the boundary and will be discussed in more detail in the section on NUMERICAL APPROACH.

Zero Gradient Distribution Function

The momentum equation for Couette flow with zero pressure gradient in the continuum theory for turbulence reduces to a statement that total stress is constant between the plates. If attention is confined to the region well outside the viscous sublayer, then the viscous stress contribution is negligible and therefore Reynolds stress is constant. Assuming that the apparent viscosity coefficient is linear in y then gives the familiar logarithmic result for the mean velocity profile. Further, the kinetic energy of turbulence, U^2, is known to be approximately constant in such a logarithmic region[12]. In terms of the moments described earlier, these conditions give

$$\iiint_{-\infty}^{\infty} \left(c_x^2 + c_y^2 + c_z^2\right) f \, dc_x \, dc_y \, dc_z = 3U^2 = \text{constant}$$

$$\iiint_{-\infty}^{\infty} c_x \, c_y \, f \, dc_x \, dc_y \, dc_z = \overline{c_x c_y} = \text{constant}$$

Therefore, under the assumption of a linear variation in ν_T for the Couette flow problem, it should be possible to construct a boundary condition for the distribution function which causes the governing statistical equation to yield a logarithmic solution between the plates. A necessary condition for

this is to forbid f to have a gradient at the boundary point and to require it to match the law of the wall there.

The governing equation itself may be used to develop an appropriate form for f by setting $\partial f/\partial y = 0$ in Eq. (4). If one then assumes $du/dy = 1/\kappa y$, $U = U_B$, $\epsilon = du/dy$, and $1/\tau = K\,\epsilon/U^2$, the equation becomes

$$-3\,c_y\,U_B^2\,\frac{\partial f_B}{\partial c_x} = 3K(F_B - f_B) + 3f_B + c_x\frac{\partial f_B}{\partial c_x} + c_y\frac{\partial f_B}{\partial c_y} + c_z\frac{\partial f_B}{\partial c_z} \tag{10}$$

where the pressure gradient and viscous stress have been taken as zero. The subscript B is used to indicate that the distribution function obtained from solving this equation is to be employed as a boundary condition for solution to Eq. (4) for the region between the plates.

Again, it is found to be easier to work with the reduced distribution functions. The equations for these which correspond to Eq. (10) are

$$3K(G_B - g_B) + g_B + c_y\,\frac{dg_B}{dc_y} = 0 \tag{11a}$$

$$3K(J_B - j_B) + c_y\,\frac{dj_B}{dc_y} = 3g_B\,c_y\,U_B^2 \tag{11b}$$

$$3K(H_B - h_B) - h_B + c_y\,\frac{dh_B}{dc_y} = 6\,j_B\,c_y\,U_B^2 \tag{11c}$$

Solutions to these equations are independent of y and are to be applied as boundary condition functions in solving Eqs. (6). It should be noted that $\partial j_v/\partial y \neq 0$ since the mean velocity is not constant, but logarithmic. However, j_v can be related to g and j by

$$j_v = \int_{-\infty}^{\infty}\int (c_x + u)\ f\ dc_x\ dc_z = \int_{-\infty}^{\infty}\int c_x\ f\ dc_x\ dc_z + u \int_{-\infty}^{\infty}\int f\ dc_x\ dc_z$$

or

$$j_v = j + u\ g \tag{12}$$

Hence, at the boundary

$$j_{v_B} = j_B + u_B\ g_B$$

where u_B is determined by the logarithmic relation

$$u_B = \frac{u_*}{\kappa}\ \ell n \left(\frac{u_* y}{\nu}\right) + B u_*$$

with κ and B as constants. A value for $y_* = u_* y/\nu$ of 100 is used to insure that viscous stresses are, in fact, negligible at the boundary point.

The solution to the set of equations (11) must be obtained numerically. Since the distribution functions and all their velocity gradients must approach zero as $|c_y| \to \infty$, this is used as a boundary condition in velocity space. The integration proceeds from a large value of c_y toward zero and from a small negative value c_y (with large absolute value) toward zero. A first order finite difference scheme is utilized for the integration. The result of the integration is a set of numerical values for f_B which is then employed as a boundary condition in the solution of the model equation for $y_* > 100$.

Chapman-Enskog Distribution Function

There are two shortcomings in the use of the $\partial f/\partial y = 0$ boundary condition. One is that the value of u_* must be specified a priori. This is equivalent to establishing the wall shear stress, which is a quantity which hopefully would emerge from the solution rather than be required as an input in order to obtain a solution. The second is that experimental data for mean velocity may not follow the logarithmic variation throughout the entire region between solution boundaries. This point will be discussed later in the RESULTS section.

Therefore, it was desirable to seek a boundary condition for the distribution function which would circumvent these difficulties. Upon first inspection it would seem possible to impose a Gaussian distribution for f_B in a manner analogous to the use of Maxwellian re-emission of molecules from a surface in the kinetic theory of gases. However, since a Gaussian distribution function gives zero Reynolds stress, this is inappropriate for application within a turbulent zone. (There may be merit in attempting to apply the statistical model equation within the viscous sublayer, where Reynolds stresses are small and then imposing the Gaussian distribution in a limiting Dirac delta function form at some point in this region. However, this possibility was not examined under the present effort).

An organized manner of obtaining a proper boundary condition is the Chapman-Enskog procedure[14]. Employing this method one can obtain approximate solutions to Eq. (1) using a series expansion. The zeroth order solution gives an equilibrium Gaussian distribution, which, as mentioned previously, results in zero Reynolds stress. The first order solution is commonly termed the Chapman-Enskog distribution, and allows for a Reynolds stress to occur.

The first order Chapman-Enskog expansion for a one dimensional flow gives

$$f^{(1)} = F\left\{1 - \frac{\nu_T}{U^2}\left[\left(\frac{c^2}{2U^2} - \frac{5}{2}\right)\frac{c_y}{U^2}\frac{dU^2}{dy} + \frac{c_x c_y}{U^2}\frac{du}{dy}\right]\right\} \qquad (13)$$

where

$$F = \left(\frac{1}{2\pi U^2}\right)^{3/2} \exp\left[-\frac{(c_x^2 + c_y^2 + c_z^2)}{2U^2}\right]$$

is the Gaussian distribution. The corresponding nondimensional forms for the reduced distribution functions are

$$g^{(1)} = G - \frac{\nu_T}{R_{e_*} U^3} \frac{dU}{dy} c_y \left[\frac{1}{U^2}\left(H + c_y^2 G\right) - 5G\right] \tag{14a}$$

$$j^{(1)} = - \frac{\nu_T}{R_{e_*}} \frac{c_y}{U^2} \frac{du}{dy} G \tag{14b}$$

$$h^{(1)} = H - \frac{\nu_T}{R_{e_*} U^3} c_y \frac{dU}{dy} \left[\left(\frac{c_y^2}{U^2} H + 8 U^2 G\right) - 5H\right] \tag{14c}$$

$$j_v^{(1)} = j^{(1)} + u\, g^{(1)} \tag{14d}$$

These forms may then be applied as boundary conditions for the governing equation. Details of the application will be discussed in the chapter on NUMERICAL APPROACH.

Two-Stream Nature of Boundary Conditions

Even though a functional form is established for the boundary distribution function, f_B, the correct implementation of this form is not straightforward. If one examines the physics of the problem, it is clear that both plates contribute to the establishment of the flow; and, therefore, boundary conditions should be applied at a y_* value near each plate, giving two boundary conditions. (The symmetry condition at the centerline may be invoked to reduce

the problem to a half-space in y, but this still necessitates specifying two boundary conditions on f). Yet, if one examines the one-dimensional governing equation (Eq.(1)), it is observed that only a first-order derivative in y appears when viscous terms are neglected. It would thus appear that imposition of two boundary conditions would result in overspecifying the problem.

Experience in solving the Boltzmann equation in rarefied gas dynamics gives insight to resolving this paradox. In the molecular approach to rarefied flows one can only specify the velocity distribution function of molecules leaving a surface. The distribution function for those striking the surface is determined as a consequence of the solution. Thus, the boundary conditions possess a "two-stream" nature. The interaction of the incoming and outgoing stream is controlled through the collision or relaxation term in the model equation and through integral constraints such as the requirement that the incoming mass flux equal that for the outgoing stream.

If this concept is transposed to the present problem of turbulent Couette flow, one requires that at the boundary point near the lower plate the distribution function is specified only for positive values of c_y while for the corresponding point near the upper plate it is specified only for negative values of c_y. This is illustrated in Figure 1. Insofar as the function f is concerned, this is equivalent to imposing a single constraint for all c_y domain values while it allows the effects of each plate to be introduced into the problem. This is mathematically consistent with the first order nature of the y-derivative in the governing equation. Further, it seems plausible that such a two-stream approach is justified on a physical basis, since the turbulence motions leaving and approaching the wall region will be affected differently by the presence of the wall.

As with the case in rarefied gasdynamics, integral constraints must be imposed. The most obvious one is that

$$\iiint_{-\infty}^{\infty} f \, dc_x \, dc_y \, dc_z = 1$$

since this must hold from the definition of f. Additional constraints will be discussed in the chapter on NUMERICAL APPROACH.

NUMERICAL APPROACH

Discrete Ordinate Method

The discrete ordinate method is a numerical technique of replacing a continuous independent variable in a system of integro-partial differential equations by a set of discrete values and then treating these as parameters in the remaining solution. Although not restricted to integro-differential equations, the method has proven quite useful in attacking this type of problem. Two examples of this application in physics are radiative heat transfer[15] and rarefied gas dynamics[9-10]. The latter field is closely related to the present study of turbulence since a fundamental equation in rarefied gas dynamics is the Boltzmann equation for the velocity distribution function of molecules. If the BGK model is substituted for the collision integral of that equation, the one-dimensional form (which would correspond to a Couette flow geometry, for example) becomes

$$c_y \frac{\partial f}{\partial y} = -\frac{1}{\tau}(F - f)$$

in the absence of external forces. This equation possesses a form similar to Eq. (4). However, the latter equation is more complex to treat since it includes terms involving $\partial f/\partial \vec{c}$. Thus, one of the important extensions of the discrete ordinate method as applied to the present problem has been the treatment of derivatives in velocity space. Interestingly enough, the presence of external force terms in the Boltzmann equation would introduce derivatives of this type so that knowledge gained in the present numerical solution for turbulence can be transferred back to rarefied gasdynamics.

Since the moments required to compute flow properties of interest are obtained as integrals over velocity space (cf. Eqs. (8)), it is the velocity variable which is chosen to be discretized. The set of points selected is denoted by $\{c_\sigma\}$, and a continuous function, say, $g(y,c_y)$ is replaced by a set of functions $g_\sigma(y)$, $\sigma = 1,2, \ldots, S$. The same procedure is applied to each of the dependent variables. The integrations over c_y to form moments may then be accomplished by numerical quadrature employing appropriate weighting functions,

$$\int_{-\infty}^{\infty} \phi(c_y)\, g(y, c_y)\, dc_y \cong \sum_{\sigma=1}^{S} \phi(c_\sigma)\, g_\sigma(y)\, W_\sigma \qquad (15)$$

where ϕ is a function of c_y, and W_σ are the weights in the quadrature. The details of the resulting equations are shown in Appendix A.

Finite Difference Methods

Since derivatives with respect to both y and c_y are first order, the first approach taken in forming finite difference equations from the differential equations was to use simple forward or backward differences, depending upon the direction of integration. However, this first order scheme resulted in some numerical error in the region near the wall. This is illustrated in Figure 2 for the solution obtained for Reynolds stress with the $\partial f/\partial y = 0$ boundary condition. It is expected that $\overline{c_x c_y}$ should remain constant in the turbulent zone between the plates. As seen in this figure the deviation from a constant value is approximately one per cent. Although in most cases this is quite adequate in terms of accuracy, it was the non-constancy of the Reynolds Stress - as opposed to the absolute error - that was of some concern. The results for the Chapman-Enskog boundary condition show a similar, but exaggerated, behavior in that $\overline{c_x c_y}$ varied approximately fifteen percent across the turbulent zone of the channel. Some of this variation is likely due to the model assumed for the boundary condition; however, it was deemed important to reduce numerical errors so that effects of physical modeling and numerical modeling could be more clearly delineated.

Therefore, the possibility of employing a more accurate finite difference form was investigated. If a function $f(y, c_y)$ is expanded in a Taylor series about a point (y_i, c_σ), one may write

$$f_{i-1,\sigma} = f_{i,\sigma} - \left(\frac{\partial f}{\partial y}\right)_{i,\sigma} \Delta y + \frac{1}{2}\left(\frac{\partial^2 f}{\partial y^2}\right)_{i,\sigma} (\Delta y)^2 - \frac{1}{6}\left(\frac{\partial^3 f}{\partial y^3}\right)_{i,\sigma} (\Delta y)^3 + \ldots$$

and

$$f_{i-2,\sigma} = f_{i,\sigma} - 2\left(\frac{\partial f}{\partial y}\right)_{i,\sigma}(\Delta y) + \frac{4}{2}\left(\frac{\partial^2 f}{\partial y^2}\right)_{i,\sigma}(\Delta y)^2 - \frac{8}{6}\left(\frac{\partial^3 f}{\partial y^3}\right)_{i,\sigma}(\Delta y)^3 + \cdots$$

for a constant spacing Δy. Eliminating the second derivative terms, there results

$$4 f_{i-1,\sigma} - f_{i-2,\sigma} = 3f_{i,\sigma} - 2\left(\frac{\partial f}{\partial y}\right)_{i,\sigma}(\Delta y) + \frac{2}{3}\left(\frac{\partial^3 f}{\partial y^3}\right)_{i,\sigma}(\Delta y)^3 + \cdots$$

Solving for the first derivative gives

$$\left(\frac{\partial f}{\partial y}\right)_{i,\sigma} = \frac{3f_{i,\sigma} - 4f_{i-1,\sigma} + f_{i-2,\sigma}}{2\Delta y} + O\left[(\Delta y)^2\right]$$

Thus, this backward difference scheme has a truncation error of order $(\Delta y)^2$ as compared to that of order (Δy) for the simple forward difference. A similar form for a second order forward difference scheme can be developed, yielding

$$\left(\frac{\partial f}{\partial y}\right)_{i,\sigma} = \frac{4f_{i+1,\sigma} - f_{i+2,\sigma} - 3f_{i,\sigma}}{2\Delta y} + O\left[(\Delta y)^2\right]$$

In the implicit finite difference scheme employed, the distribution function and its derivative with respect to y are to be evaluated at the same grid point. Consequently, the finite difference formulae shown above are more appropriate than the usual central difference scheme.

A similar approach can be employed for deriving expressions for $\left(\partial f/\partial c_y\right)_{i,\sigma}$. However, the spacing of discrete velocity points is necessarily variable so that efficient use of quadrature can be achieved. Therefore, it is preferable to obtain a second order finite difference expression from a Lagrange interpolation formula[16]. This results in the following differences:

$$\text{(backward)} \quad \left(\frac{\partial f}{\partial c_y}\right)_{i,\sigma} = \frac{(c_\sigma - c_{\sigma-1})}{(c_{\sigma-2} - c_{\sigma-1})(c_{\sigma-2} - c_\sigma)} f_{i,\sigma-2} \tag{15a}$$

$$+ \frac{(c_\sigma - c_{\sigma-2})}{(c_{\sigma-1} - c_{\sigma-2})(c_{\sigma-1} - c_\sigma)} f_{i,\sigma-1}$$

$$+ \frac{2c_\sigma - c_{\sigma-1} - c_{\sigma-2}}{(c_\sigma - c_{\sigma-2})(c_\sigma - c_{\sigma-1})} f_{i,\sigma}$$

$$+ 0\left[\left(\Delta c_\sigma\right)^2\right]$$

$$\text{(forward)} \quad \left(\frac{\partial f}{\partial c_y}\right)_{i,\sigma} = \frac{(2c_\sigma - c_{\sigma+1} - c_{\sigma+2})}{(c_\sigma - c_{\sigma+1})(c_\sigma - c_{\sigma+2})} f_{i,\sigma} \tag{15b}$$

$$+ \frac{(c_\sigma - c_{\sigma+2})}{(c_{\sigma+1} - c_\sigma)(c_{\sigma+1} - c_{\sigma+2})} f_{i,\sigma+1}$$

$$+ \frac{(c_\sigma - c_{\sigma+1})}{(c_{\sigma+2} - c_\sigma)(c_{\sigma+2} - c_{\sigma+1})} f_{i,\sigma+2}$$

$$+ 0\left[\left(\Delta c_\sigma\right)^2\right]$$

As a consequence of the two-stream nature of the distribution functions, the choice of the difference scheme (either forward or backward) is readily prescribed. For the "positive" stream ($c_\sigma > 0$), the computations should proceed from $+\infty$ (where boundary conditions with respect to velocity space are known) to zero and from the lower boundary point (where conditions with respect to physical space are known) to the upper boundary. Thus, the forward difference in velocity space and the backward difference in physical space are employed. For the "negative" stream ($c_\sigma < 0$) the reverse is true. There, the integration proceeds from $-\infty$ to 0 in c_y and from upper boundary to lower boundary in y. Thus, the backward difference in velocity space and the forward difference in physical space are utilized. When these forms are substituted for the derivative terms in Eqs. (9), a set of difference equations for the reduced distribution functions is obtained. These equations are given in detail in Appendix B.

Iterative Scheme

The resulting equations must be solved by an iteration process since they contain terms which depend upon the macroscopic properties. Therefore, initial guesses are made for u, U, and ϵ (an initial profile for Reynolds stress is not required). The equations for the "positive stream" are then solved from the boundary point up to the centerline, symmetry conditions are applied, and the "negative stream" is then computed from centerline to boundary point. This completes one iteration and yields the approximation to the reduced distribution functions. From these, new profiles for the macroscopic quantities are found and stored for use in the second iteration. If integral constraints are required at the boundary point, these are imposed before the second iteration is begun. These will be discussed in the next section.

This iterative process continues until satisfactory convergence is obtained for the macroscopic properties.

Constraints at Boundary

The form of the distribution at the boundary point dictates the constraints which must be applied.

Zero Gradient Boundary Condition. In employing the boundary condition found from setting $\partial f/\partial y = 0$, it is necessary to specify U and u_* (hence, the value of the wall shear stress). This is the value of u_* that would result if the mean velocity were logarithmic between the plates. Equations (11) are then solved, subject to these constraints, to give the boundary conditions on g, j, h. These conditions are then fixed for all iterations. The values of u and du/dy at the boundary point are determined from the law of the wall, utilizing the assumed value of u_*.

Chapman-Enskog Boundary Conditions. As discussed, the Chapman-Enskog form of the distribution function may be used as a boundary condition on the positive stream. With this form it is possible to deduce the value of wall shear from the solution to the equations, rather than requiring an a priori assumption on u_*. This is achieved by applying appropriate integral constraints upon the outgoing and incoming streams at the boundary point. If the Chapman-Enskog forms are written for the reduced distribution functions, there results

$$g^{(1)} = G - \frac{\nu_T}{Re_* U^3} \frac{dU}{dy} c_y \left[\frac{1}{U^2} (H + c_y^2 G) - 5G \right] \tag{16a}$$

$$j^{(1)} = - \frac{\nu_T}{Re_*} \frac{c_y}{U^2} \frac{du}{dy} G \tag{16b}$$

$$h^{(1)} = H - \frac{\nu_T}{Re_* U^3} c_y \frac{dU}{dy} \left[\left(\frac{c_y^2}{U^2} H + 8 U^2 G \right) - 5H \right] \tag{16c}$$

$$j_v^{(1)} = j^{(1)} + u\, g^{(1)} \tag{16d}$$

Using these equations as boundary conditions on the outgoing or positive stream at the lower boundary point, the first iteration may begin once initial guesses are posed for the macroscopic quantities. Then, upon marching back from the centerline of symmetry, certain quantities must be re-evaluated before the second iteration can proceed. These are

$$U$$

$$-\frac{\nu_T}{Re_* U^3}\frac{dU}{dy}$$

and

$$-\frac{\nu_T}{Re_*}\frac{du}{dy} = \overline{c_x c_y}$$

In the present study the following constraints have been applied:

$$\overline{c_x c_y} = -\frac{\nu_T}{Re_*}\frac{du}{dy} = -1.0 \tag{17a}$$

$$\int_{-\infty}^{\infty} g\, dc_y = \int_{-\infty}^{0} g^- dc_y + \int_{0}^{\infty} g^+ dc_y = 1.0 \tag{17b}$$

$$\bar{c}_y = \int_{-\infty}^{\infty} c_y\, g\, dc_y = \int_{-\infty}^{0} c_y\, g^-\, dc_y + \int_{0}^{\infty} c_y\, g^+\, dc_y = 0 \tag{17c}$$

The first of these states that the Reynolds stress at the boundary point is equal to the wall shear stress (the viscous stress could be included in this equation and, in fact, several calculations have been performed over the course

of the study in which this has been done). The second condition states that the probability of finding a fluid element with velocity between $-\infty$ and $+\infty$ is unity, while the third requires that the time average of the fluctuating vertical velocity component be zero.

If the Chapman-Enskog forms of Eqs. (16) are substituted into Eqs. (17b,c), there results

$$\frac{\nu_T}{Re_* U^3} \frac{dU}{dy} = \sqrt{2\pi} \frac{(0.5 - c_1)}{U} \tag{18a}$$

and

$$U = -\sqrt{2\pi}\ c_2 \tag{18b}$$

where

$$c_1 = \int_{-\infty}^{0} g^- \, dc_y$$

and

$$c_2 = \int_{-\infty}^{0} c_y \, g^- \, dc_y \, .$$

The latter two integrals are computed numerically at the end of each iteration, based upon the current iterate for the g^- (or incoming stream) distribution. Thus, parameters in the outgoing stream may be readjusted at each iteration to conform with the imposed constraints. The value for u_*, and hence wall shear stress, is obtained by requiring that the computed value of u at the boundary point fit the logarithmic relation for law of the wall,

$$u = \frac{1}{\kappa} \ln\left(\frac{u_* y}{\nu}\right) + B$$

It is emphasized that this is the only point, under this Chapman-Enskog scheme for boundary conditions, at which law of the wall is assumed to hold; and this is implemented only to avoid using the statistical model for turbulence within the region where viscous stresses are comparable to or larger than Reynolds stresses.

RESULTS

All calculations reported here for the present study were made at a Reynolds number ($Re = u_w d/\nu$) of 17,000.

Zero-Gradient Boundary Condition

The motivation for deriving this boundary condition and applying it to the Couette flow problem was twofold. First, it was important to determine whether, under appropriate assumptions, the statistical model equation could reproduce a turbulent flow within which the mean velocity varied logarithmically and the Reynolds stress remained constant. Since it is known from experiments that such a region exists near the wall for many turbulent flows, the capability of the model to recover this result is a logical first test of its validity. Second, it was expected that such a boundary condition might potentially be applied to more general situations than the Couette flow due to, as mentioned above, the existence of a limited logarithmic region for many boundary layer flows.

So that the expression for ϵ in the statistical model equation is consistent with the law of the wall in the logarithmic region, the production is set equal to the dissipation, giving[17]

$$\epsilon = 0.7968\ U^3/y \tag{19}$$

The zero gradient boundary conditions obtained from the numerical solution to Eqs. (11) and the equation for ϵ, Eq. (19), were applied to the equations for Couette flow, Eqs. (9). The numerical scheme was that of second order finite differences derived in the previous section. An initial guess for mean velocity which corresponded to the law of the wall variation was assumed, and the iterative process was begun. Constants in the logarithmic mean velocity profile were taken as $\kappa = 0.41$ and $B = 5.0$[17]. After 45 iterations, the mean velocity profile had converged to and remained within 0.05 percent of the logarithmic profile; and the dimensionless Reynolds stress was constant to three significant digits at - 0.992 (exact value is - 1.0). The numerical procedure has been shown to give a unique solution for different initial guesses for the velocity profile. For example, in one case the logarithmic profile was used as an initial guess and in another a linear profile for mean velocity was employed. The converged results agreed for both examples.

Solutions obtained using the zero gradient boundary condition have clearly demonstrated that the Lundgren's model equation is a reasonable one and have given encouragement that accurate results may be obtained from such a statistical approach. Further, it is believed that these results have demonstrated the numerical accuracy of the discrete ordinate and difference schemes presently employed.

Chapman-Enskog Boundary Condition

Although it is established that a logarithmic region exists near the wall for many boundary layer flows, this does not imply that such a region will extend across the entire field for the Couette flow case. In fact, experimental data indicate that such may not be the situation[12,13]. Although Johnson's[18] data for Couette flow can be made to fit the law of the wall if $\kappa = 0.4115$ and $B = 5.6$, the fact that these "constants" may not fit other experimental data indicates a lack of rigor in specifying a unique result. Furthermore, Reichardt's[13] data for mean velocity do not fit a logarithmic variation very well for any pair of these constants.

If the experimental value of u_* quoted by Reichardt is employed and reasonable values of κ and B are assumed, the logarithmic velocity profile does not pass through zero at the centerline and does not fit the experimental data well. On the other hand, by selecting a rather large value of B (7.456) the logarithmic profile can be made to satisfy zero velocity at the centerline, but this does not follow the experimental data elsewhere.

The Chapman-Enskog form of the distribution function for the outgoing stream was employed as a boundary condition in a series of calculations. The first results reported here were obtained with the first order difference scheme. Calculations utilizing the improved second order scheme are currently in progress and some results will be given. The major difference obtained by using these two numerical methods is improved accuracy near the boundary with the second order technique. Numerical solutions have been calculated using both the algebraic (Eq. (9e)) and differential (Eq. (9f)) equations for the dissipation ϵ. In all cases reported, the solutions were unique and convergent. This was tested by employing different initial profiles, various grid spacings, and different boundary point locations.

Figure 3 illustrates the results for mean velocity. The experimental data of Reichardt are plotted for comparison. The logarithmic profile corresponding to $\kappa = 0.41$ and $B = 5.0$ is also shown. Both of the solutions using the statistical model equation fall very near to the experimental data. The case for $\epsilon \sim U^3/y$ is particularly close. Some differences can be observed between the solution obtained assuming that dissipation equals production and that found when the differential equation for ϵ is utilized. These differences are relatively minor. Chung's solutions[16] are also plotted for comparative purposes. The ratio of friction velocity to plate velocity quoted by Reichardt was

$$\frac{u_*}{u_w} \cong 0.0425 \quad (\mathrm{Re} = 17{,}000)$$

while the calculated values were

$$\frac{u_*}{u_w} = 0.04487 \quad (\text{Using Eq. (9e) for } \epsilon \text{ ; } \mathrm{Re} = 17{,}000)$$

and

$$\frac{u_*}{u_w} = 0.04467 \quad (\text{Using Eq. (9f) for } \epsilon \text{ ; } \mathrm{Re} = 17{,}000)$$

Chung's calculated values[6] were 0.03284 (Re = 36,000) and 0.0405 (Re = 9,810).

Results for Reynolds stress are given in Figure 4. The experimental data[13,18] are shown for comparison. The calculated results show a variable Reynolds stress which decreases near the wall boundary. The decrease is not a consequence of increasing viscous stress but rather is a result of some numerical error with the first order scheme and of modelling the boundary condition using the Chapman-Enskog form. Despite this variation, the calculated results are within ± 15 per cent of the experimental values. Experience with the second order difference scheme shows substantial improvement in the Reynolds stress profile near the wall. Again, Chung's results[6] are shown for comparison.

The profiles for kinetic energy are given in Figure 5. There is very little difference between the results for the two models for ϵ, and both profiles show a slight decrease in turbulence kinetic energy as the wall boundary point is approached.

An interesting aspect of the statistical approach to turbulence is that the distribution functions may be calculated. This may offer insight into turbulence mechanisms and aid turbulence modeling. Figure 6 illustrates the g distribution employed as a boundary condition for both the zero gradient and Chapman-Enskog cases, while Figure 7 shows a similar graph for j. (It is emphasized that only the outgoing stream is modeled with these functions). The Chapman-Enskog distributions are somewhat broader than those for $\partial f/\partial y = 0$. This is particularly noticeable for the j distribution function. It should be pointed out again that a Gaussian distribution would lead to $j = 0$ for all c_y and to a zero value of Reynolds stress. It should also be pointed out here that the Chapman-Enskog distribution does not satisfy the governing differential equation at the boundary. Therefore some gradients can be expected with such an approach.

Figure 8 shows results for g at several y locations across the channel for the Chapman-Enskog boundary condition case. The two-stream nature of the distribution function when employing this boundary condition is clearly evident. Near the wall ($y = 0.125$) there is a noticeable discontinuity in g at $c_y = 0$. This discontinuity gradually decreases as y increases. This is a consequence of the influence of the relaxation term in the governing equation. Physically, the fluid elements are interacting to smooth out the distribution function.

Recently obtained results employing the Chapman-Enskog boundary condition, the differential equation model for ϵ, and the second order difference scheme are shown in Figures 9 through 13. Figure 9 illustrates the results for the mean velocity profile and compares these with Reichardt's experimental data. The comparison is quite favorable. The Reynolds stress is given in Figure 10. It can be seen that, although the calculations do not give a flat profile, the sharp decline in $\overline{c_x c_y}$ near the wall experienced with the first order scheme is substantially reduced by employing the second order difference form. The calculated value for u_*/u_w is 0.044377, compared with the value of 0.0425 deduced from Reichardt's data. The turbulence kinetic energy, shown in Figure 11, is also reasonably constant across the channel. Figure 12 illustrates the results obtained

for ϵ from Equations (9e) and (9f). The two solutions compare quite well. This indicates that the algebraic expression for ϵ, Eq. (9e), is very good for Couette flow.

Another interesting feature of the present approach is that it is also possible to compute the contribution of the y-component of velocity fluctuations to the turbulence kinetic energy. This contribution, as shown in Figure 13, is almost constant except for a slight variation near the boundary point. In regions away from the boundary point, the solution obtained shows that $\overline{c_y^2}$ is about 89 per cent of U^2. In this region, as seen from Figure 8, the distribution function, g, does not vary with Y. For such cases, it can be shown from Equation (9a) that

$$\frac{\overline{c_y^2}}{U^2} = \left(\frac{3K}{3K + 2}\right) .$$

For the value of K used in this region, this ratio is about 0.89. This ratio, however, is quite different from the isotropic value. Thus, the results obtained with the improved difference scheme are quite encouraging.

CONCLUSIONS

The present study has accomplished the following:

(i) A convergent numerical scheme employing a combination of the discrete ordinate method and finite differences has been developed for solving the one-dimensional form of Lundgren's model equation for turbulence.

(ii) Physically realistic boundary conditions for the distribution function and models for the turbulence dissipation rate have been examined.

(iii) Lundgren's equation has been proven to yield reasonable results for mean velocity, Reynolds stress, and turbulence kinetic energy for the case of simple Couette flow.

Thus, it is believed that this research has yielded important contributions to the understanding and modelling of turbulent flows; and further, that the knowledge gained provides a basis for additional studies in fundamental aspects of turbulence.

The comparisons of theory and experiment reported here indicate that the statistical approach taken by Lundgren provides an accurate description of a simple case of wall-bounded turbulence -- Couette flow with no pressure gradient. However, there are only limited experimental data available for comparison. An appropriate extension of the present work would be to consider the case of channel flow, for which more extensive measurements are published. One of the primary areas of study should be the use of such data to better model the boundary conditions for the distribution function. Further refinements in the statistical model itself should be considered if comparisons of theoretical and experimental results indicate difficulties with the basic BGK-type approach used by Lundgren. Based on the experience with Couette flow, numerical solutions should be relatively straightforward and inexpensive (in terms of computer

time) for one-dimensional problems which include pressure gradient and chemical reactions.

Computation time to achieve a converged solution for the zero-gradient boundary condition was about 12 minutes on a UNIVAC 1108. For the Chapman-Enskog boundary condition, total computation time varied from 25 to 50 minutes, depending on the choice of initial profiles.

Although the numerical techniques would be more complex and time-consuming, certain simple two-dimensional problems could also be attacked using the model equation and solution method employed in the present research. Examples of this are free shear layers and boundary layer flows. However, it is thought that the real value in employing the statistical approach to turbulent flows examined here is in furthering basic understanding, as opposed to developing a practical computational tool.

REFERENCES

1. T. S. Lundgren, Physics of Fluids, Vol. 10, 5, p. 969, (1967).
2. P. M. Chung, AIAA Journal, Vol. 7, p. 1982 (1969).
3. E.G.D. Cohen, Fundamental Problems in Statistical Mechanics, (North-Holland Publishing Company, Amsterdam, 1972), p. 110.
4. T. S. Lundgren, Physics of Fluids, Vol. 12, No. 3, p. 485 (1969).
5. P. L. Bhatnagar, E. P. Gross, and M. Krook, Physical Review, Vol. 94, p. 511 (1954).
6. P. M. Chung, "A Turbulence Description of Couette Flow", Report TR-E-39, College of Engineering, University of Illinois at Chicago Circle (1971).
7. P. M. Chung, Physics of Fluids, Vol. 13, No. 5, p. 1153, (1970).
8. H. M. Mott-Smith, Physical Review, Vol. 82, p. 885, (1951).
9. D. P. Giddens, "Study of Rarefied Gas Flows by the Discrete Ordinate Method", Ph.D. Thesis, Georgia Institute of Technology (1967).
10. A. B. Huang, P. F. Hwang, D. P. Giddens, and R. Srinivasan, Physics of Fluids, Vol. 16, No. 6, p. 814 (1973).
11. W. P. Jones and B. E. Launder, International Journal of Heat and Mass Transfer, Vol. 15, p. 301, (1972).
12. J. M. Robertson, University of Illinois Theoretical and Applied Mechanics Report No. 141 (1959).
13. H. Reichardt, Report No. 22 of the Max-Planck-Institute für Strömungforschung and the Aerodynamische Versuchsanstalt, Göttingen (1959).
14. S. Chapman and T. G. Cowling, The Mathematical Theory of Non-Uniform Gases, (Cambridge University Press, New York, 1960), Chapter 7.
15. S. Chandrasekhar, Radiative Transfer, (Dover Publishing Company, New York, 1960).
16. M. Abramowitz and I. A. Stegun, Handbook of Mathematical Functions, (Dover Publishing Company, New York, 1965), p. 878.
17. H. Tennekes and J. L. Lumley, A First Course in Turbulence, (The MIT Press, 1972).
18. H. F. Johnson, "An Experimental Study of Plane Turbulent Couette Flow", M. S. Thesis, University of Illinois, Urbana, Illinois, (1965).

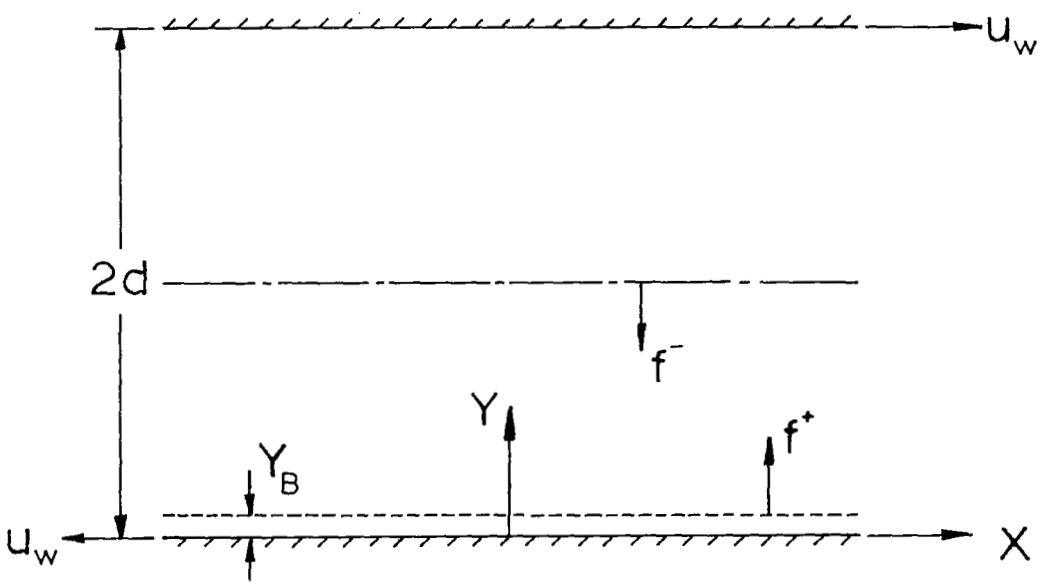

Fig. 1 Couette Flow Configuration

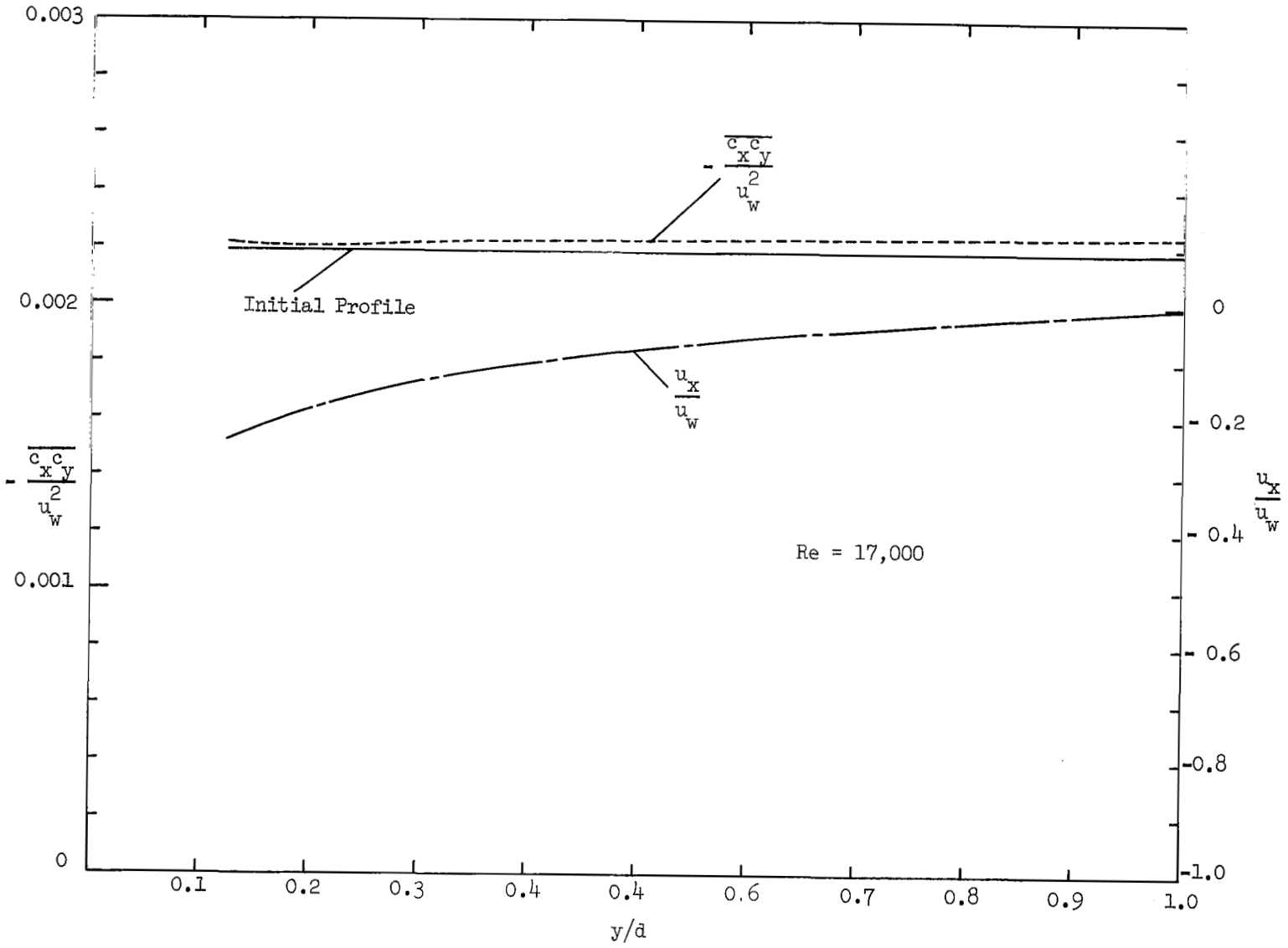

Fig. 2 First-order Difference Solutions for Zero Gradient Boundary Conditions

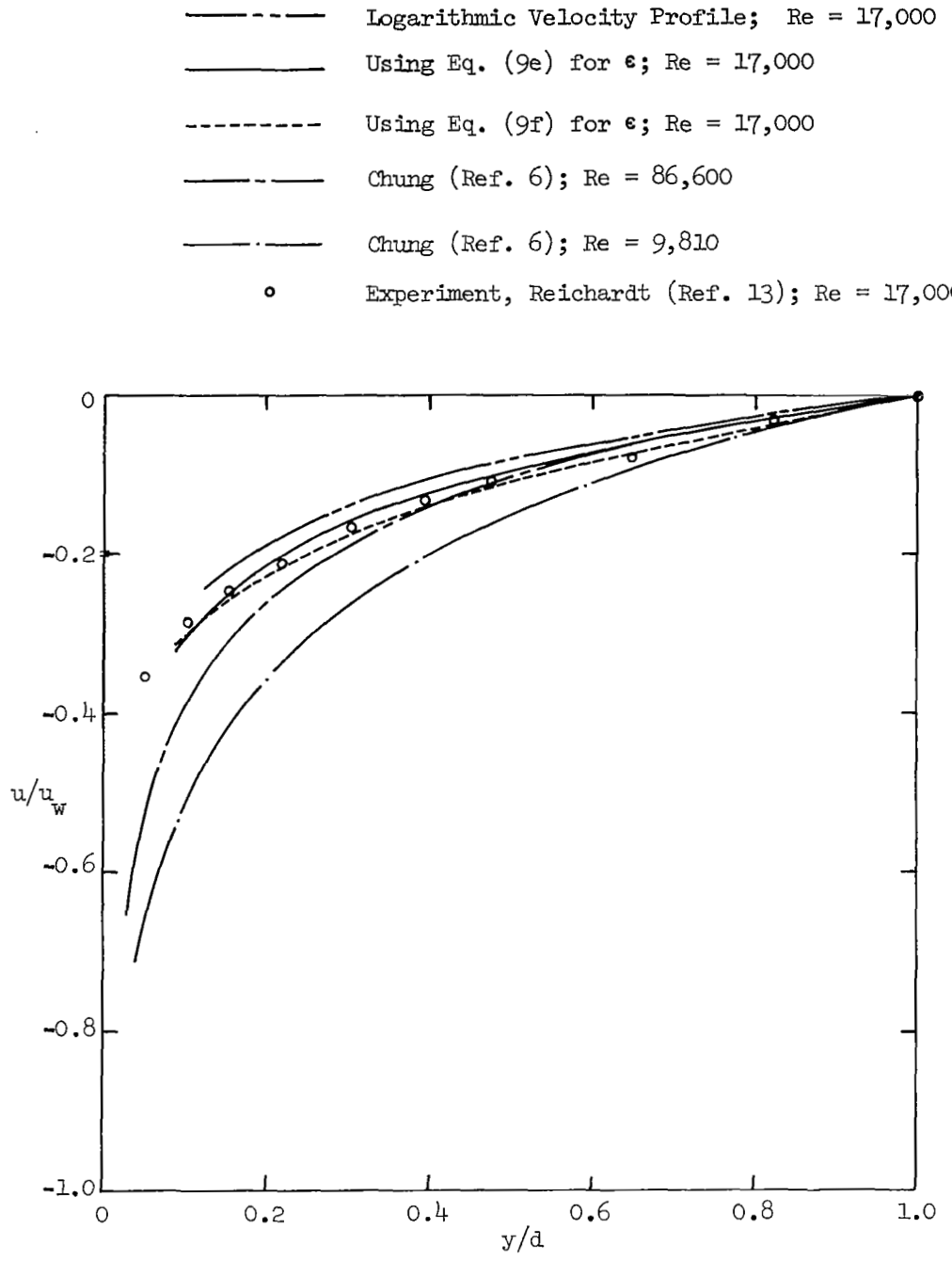

Fig. 3 Mean Velocity Profile. First-order Difference Solution

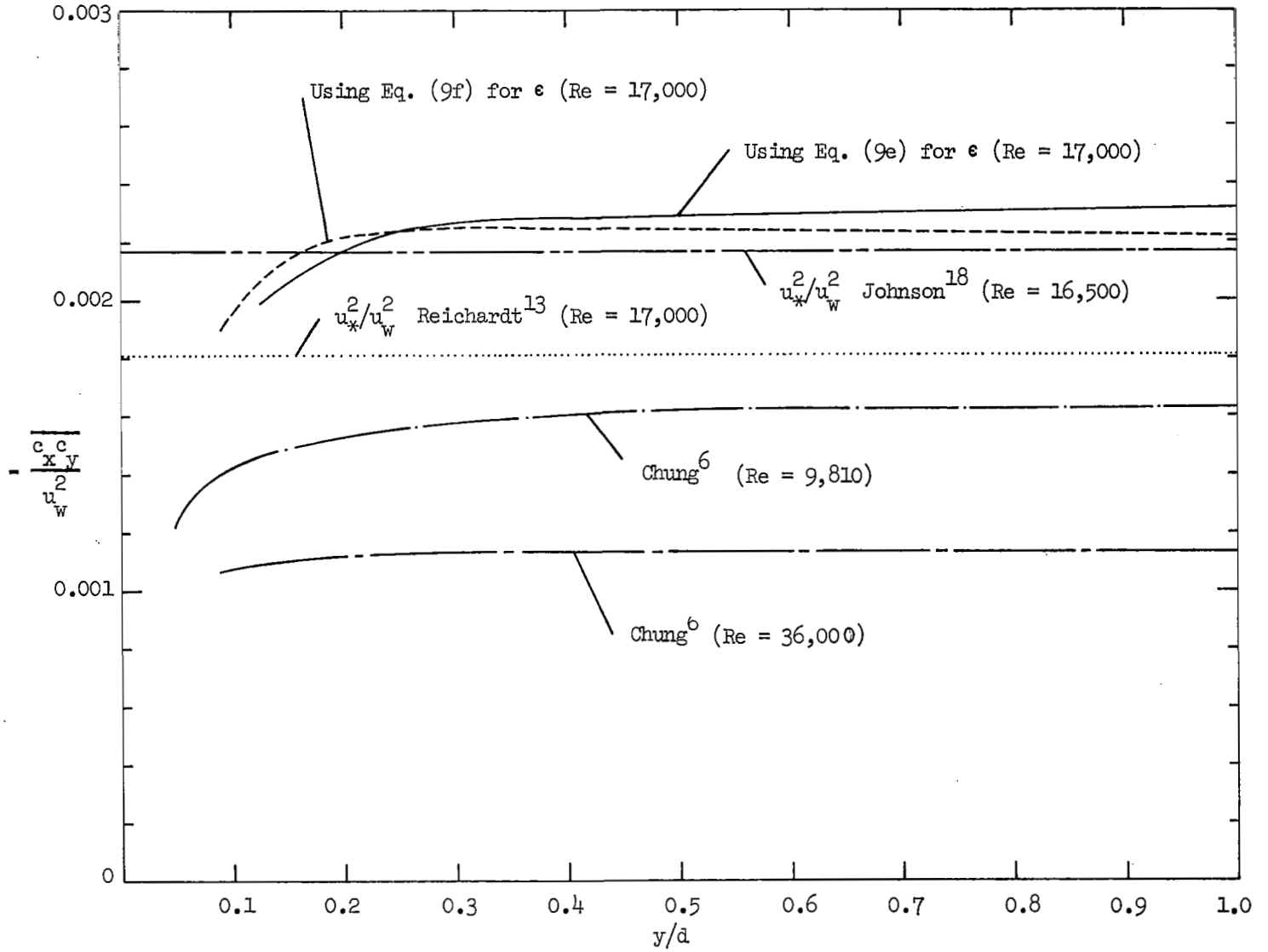

Fig. 4 Reynolds Stress Profile. First-order Difference Solution

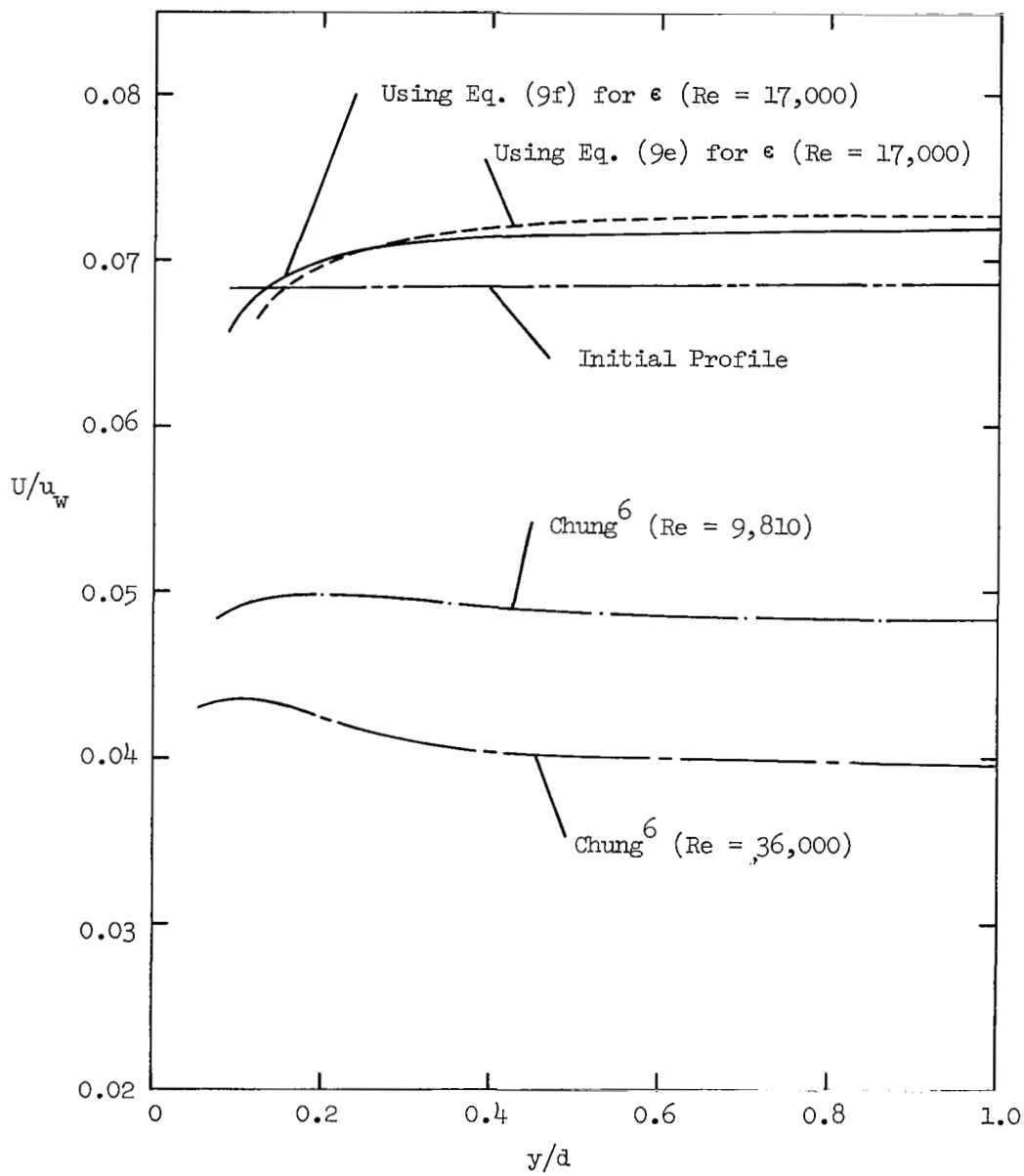

Fig. 5 Turbulence Intensity, U. First-order Difference Solution

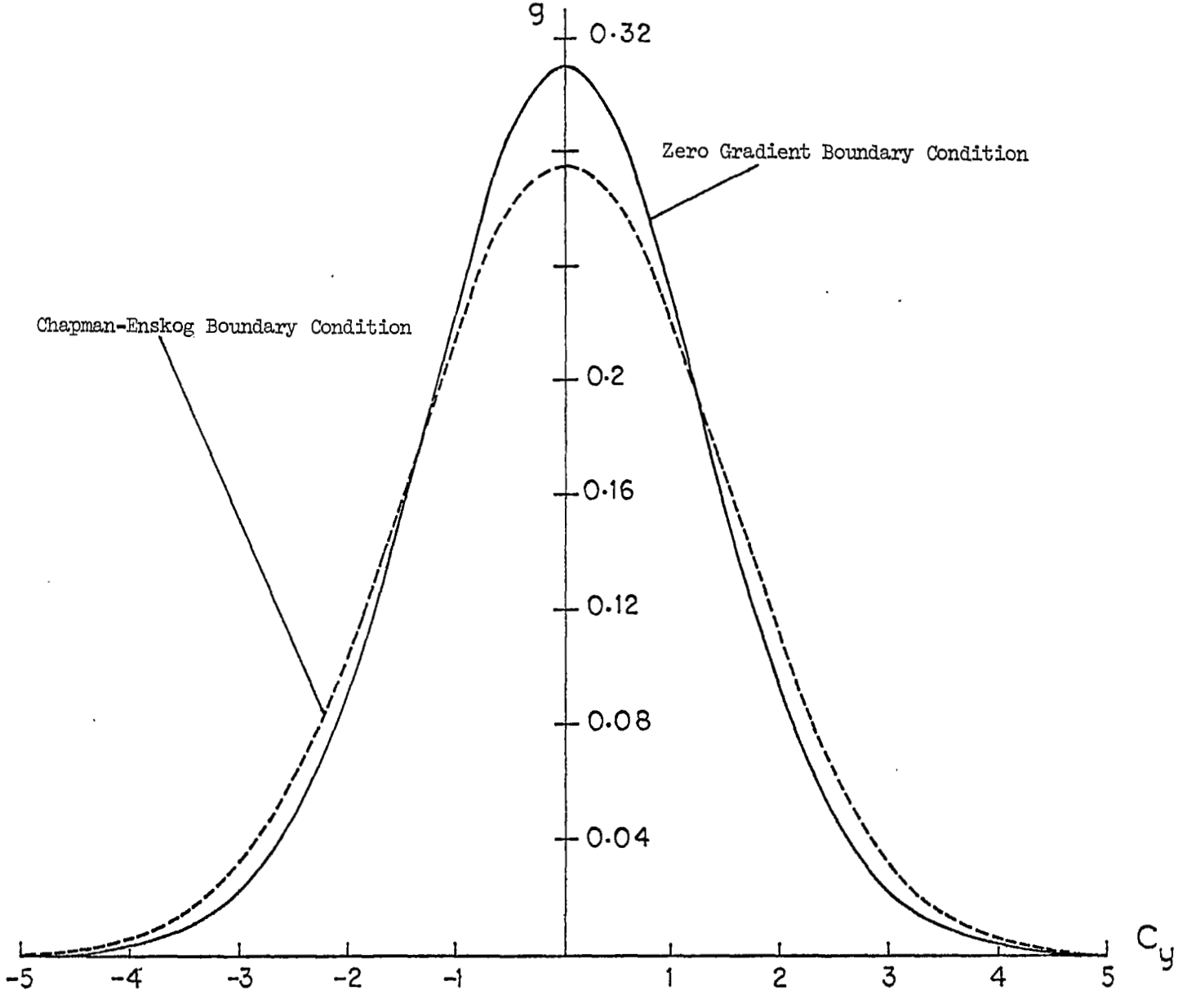

Fig. 6 Turbulence Distribution Function, g , at the Boundary Point

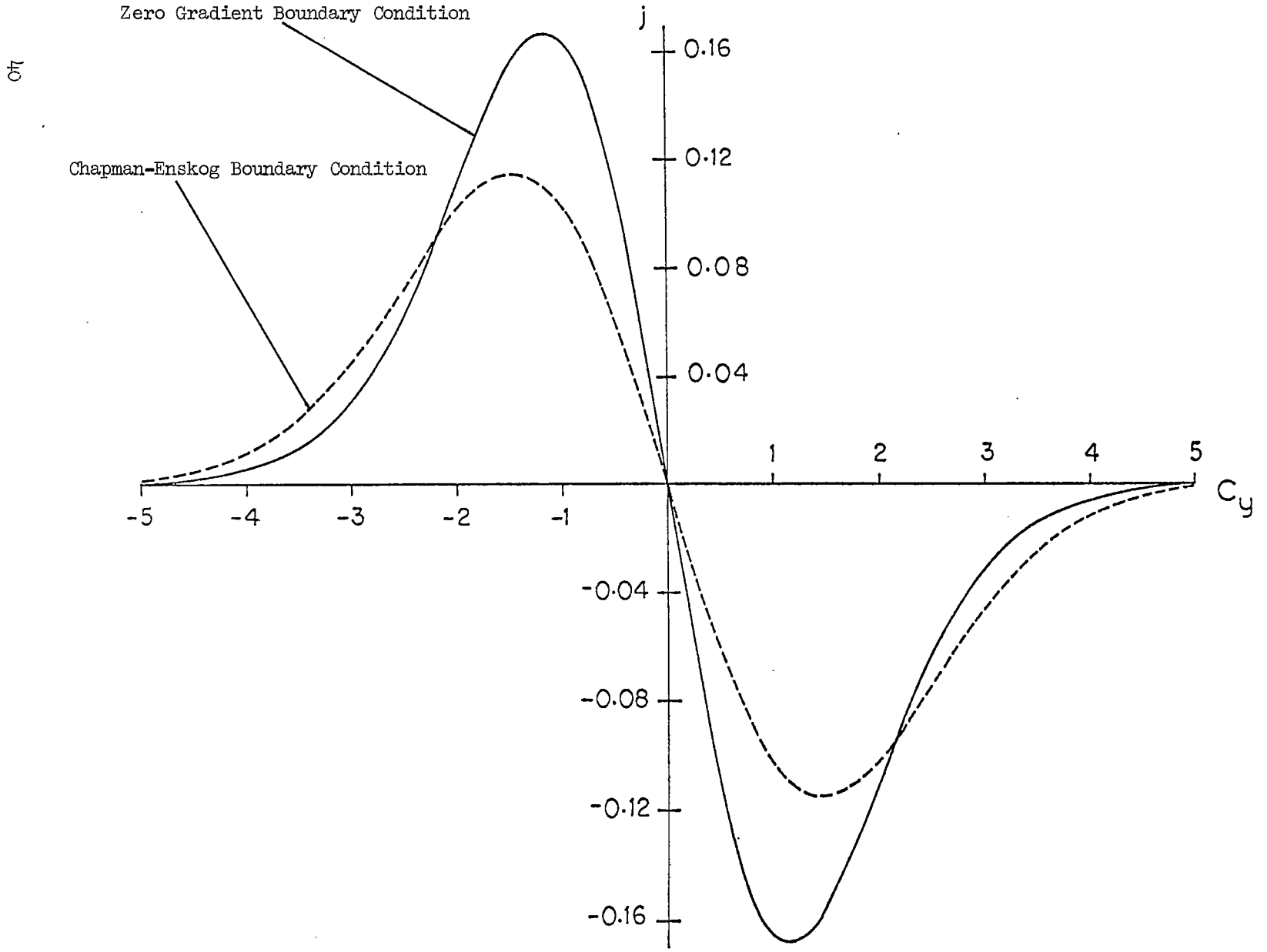

Fig. 7 Turbulence Distribution Function, j , at the Boundary Point

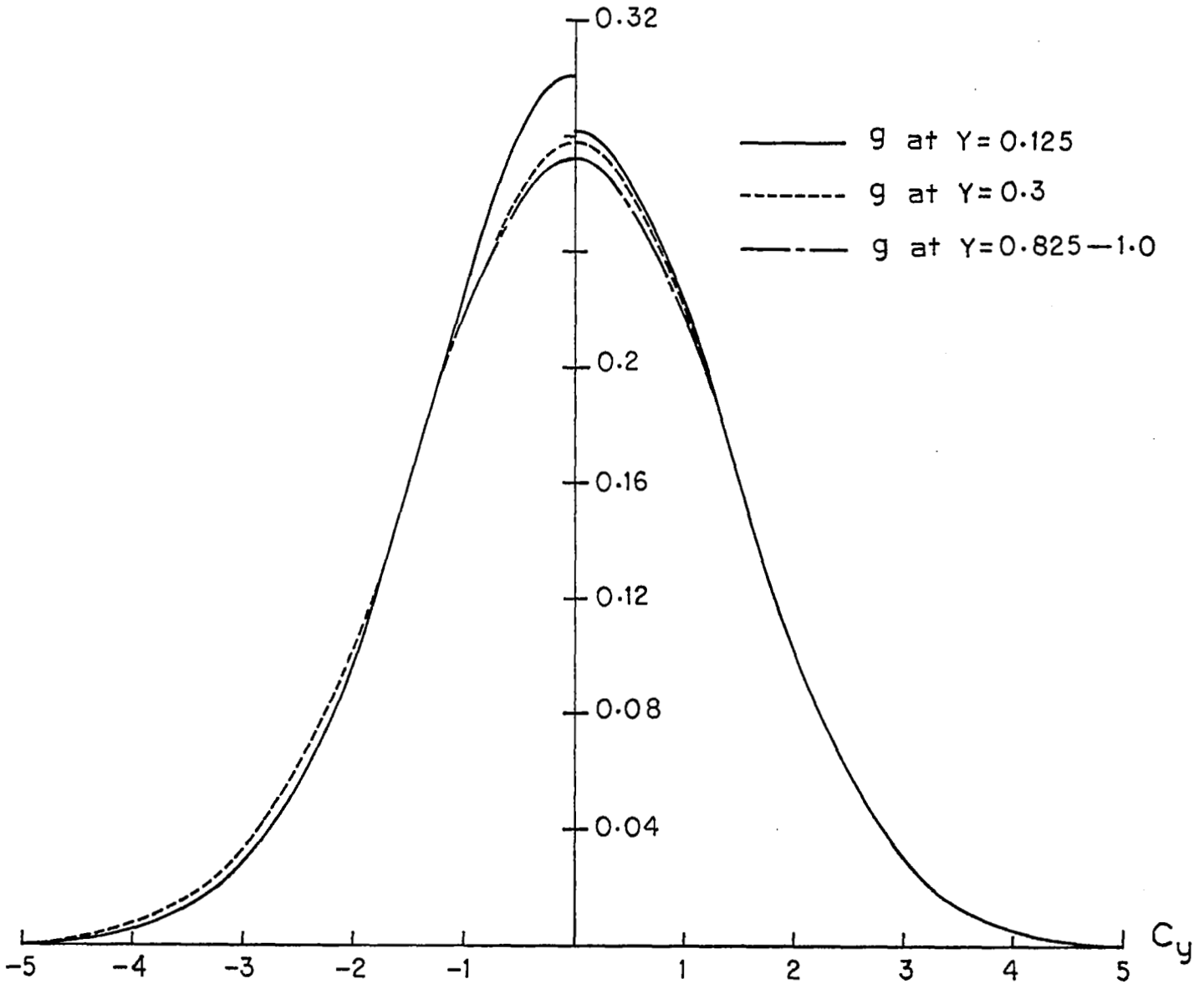

Fig. 8 Turbulence Distribution, g , for Chapman-Enskog Boundary Conditions

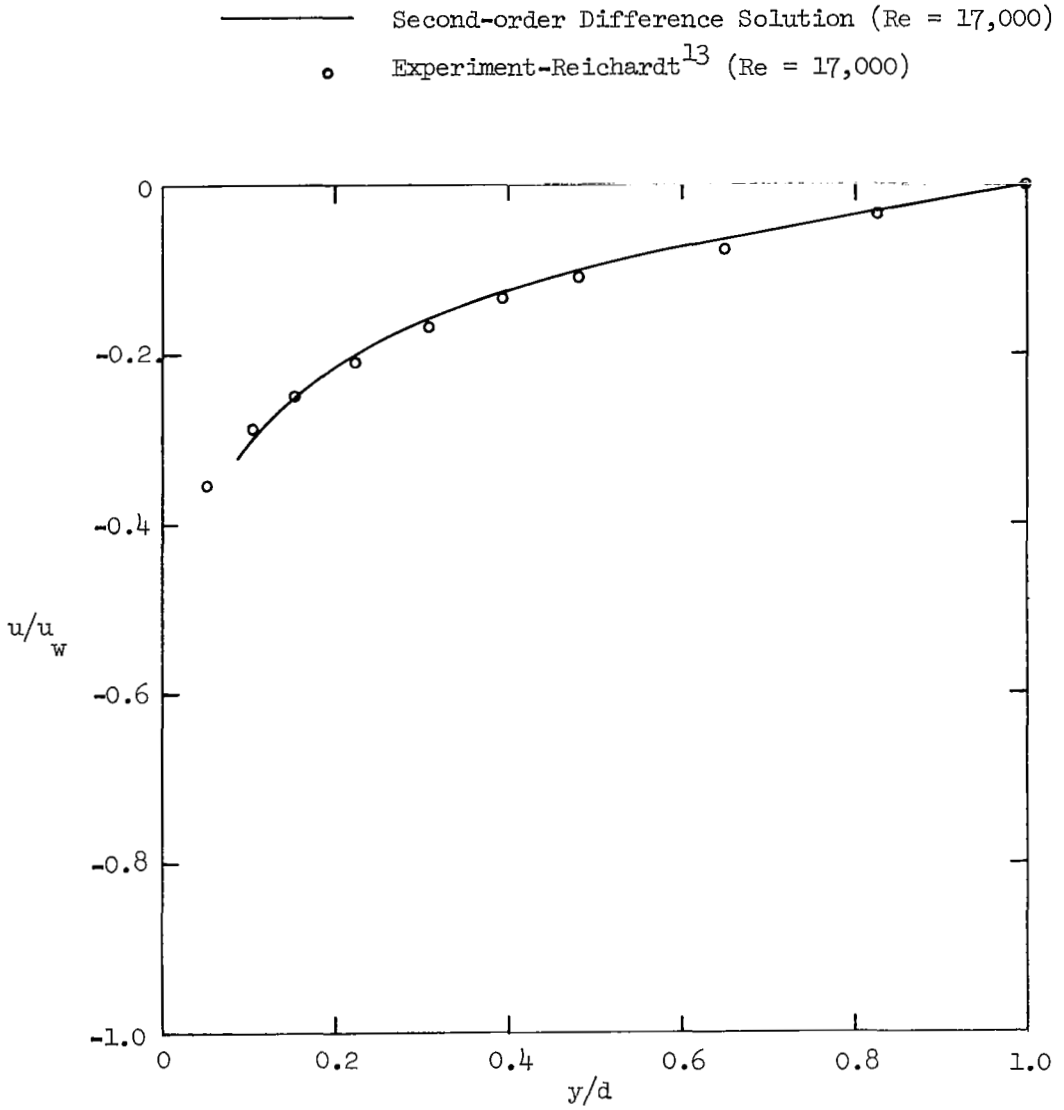

Fig. 9 Mean Velocity Profile

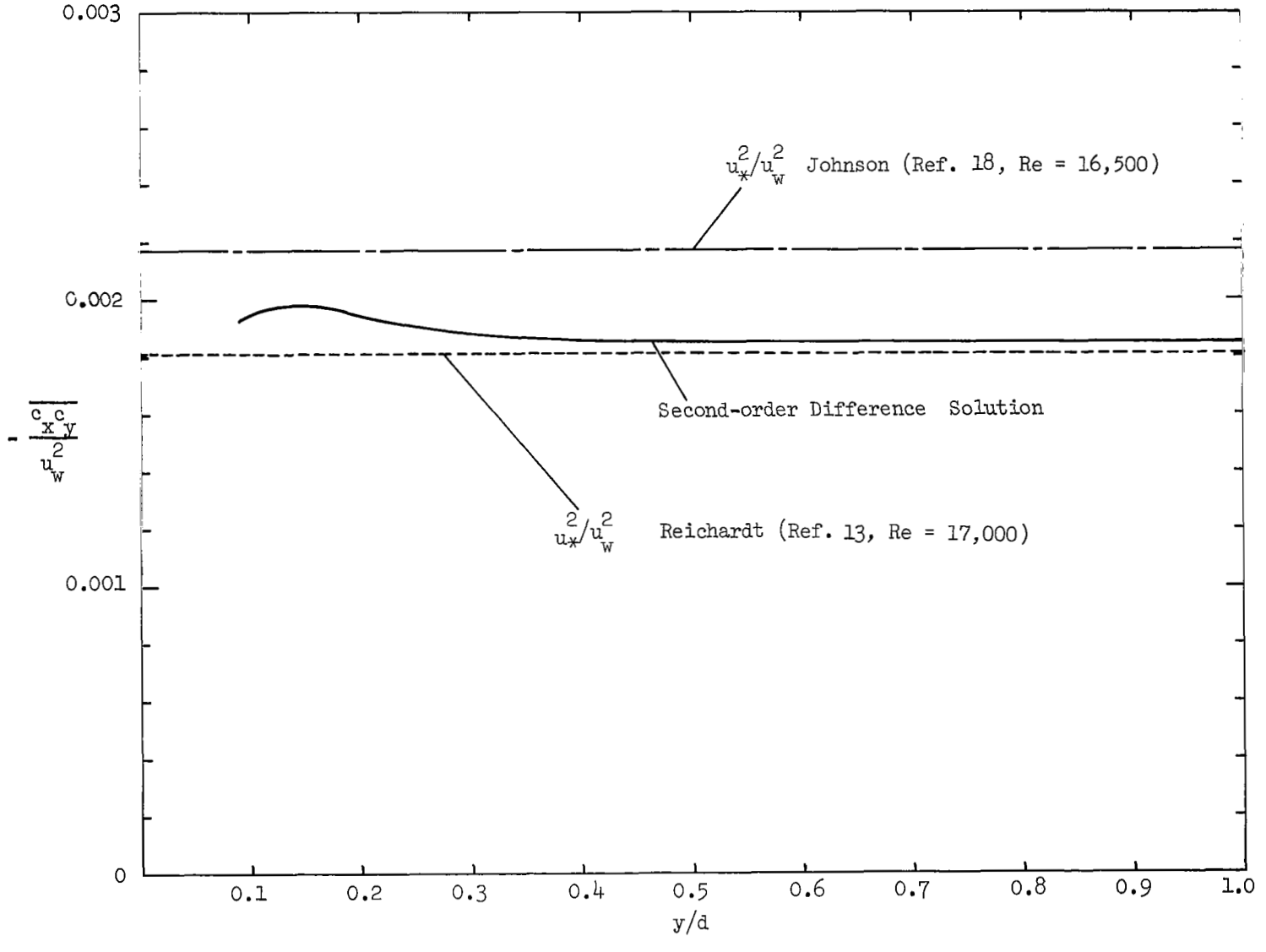

Fig. 10 Reynolds Stress Profile

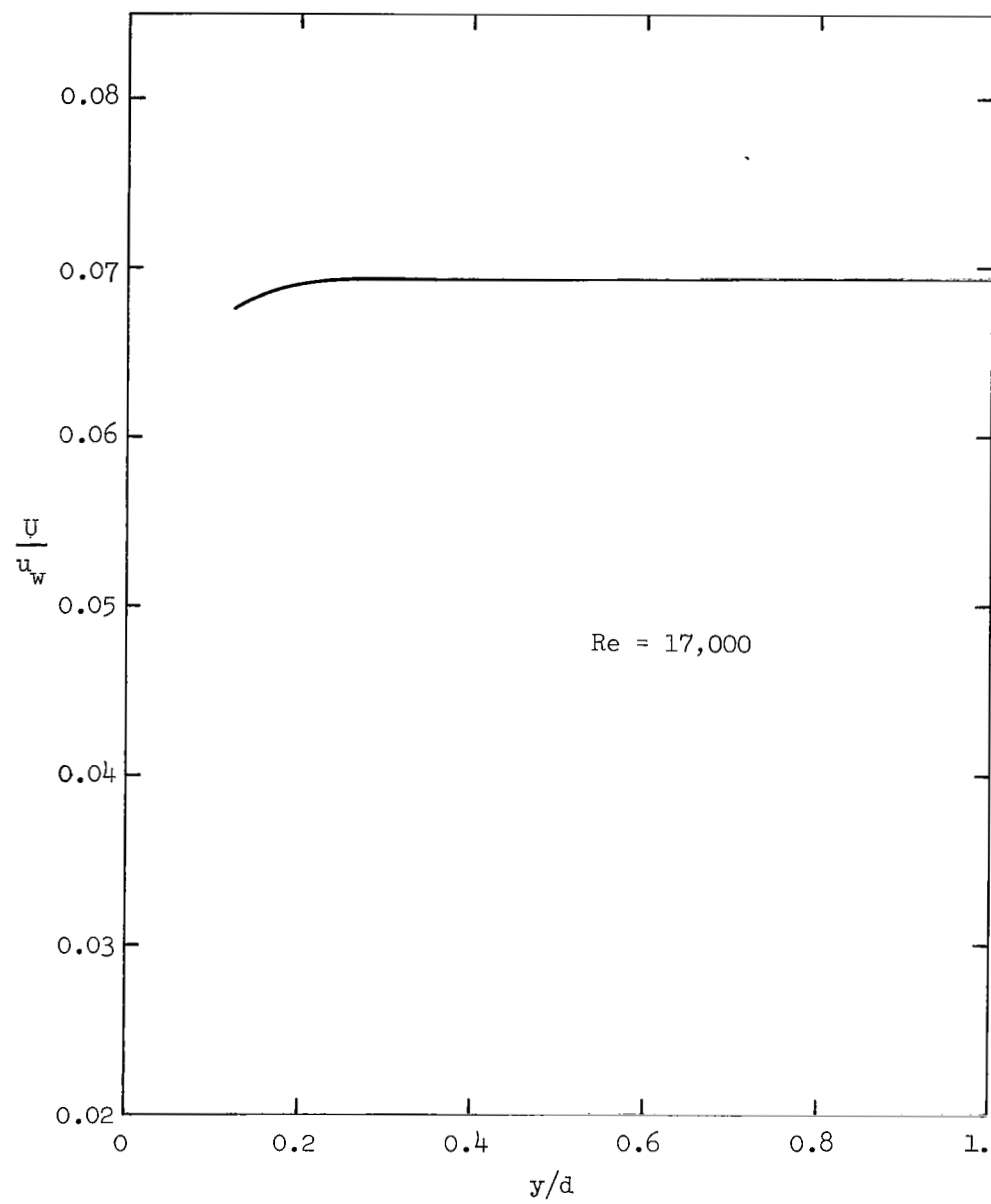

Fig. 11 Turbulence Intensity, U . Second-order Difference Solution

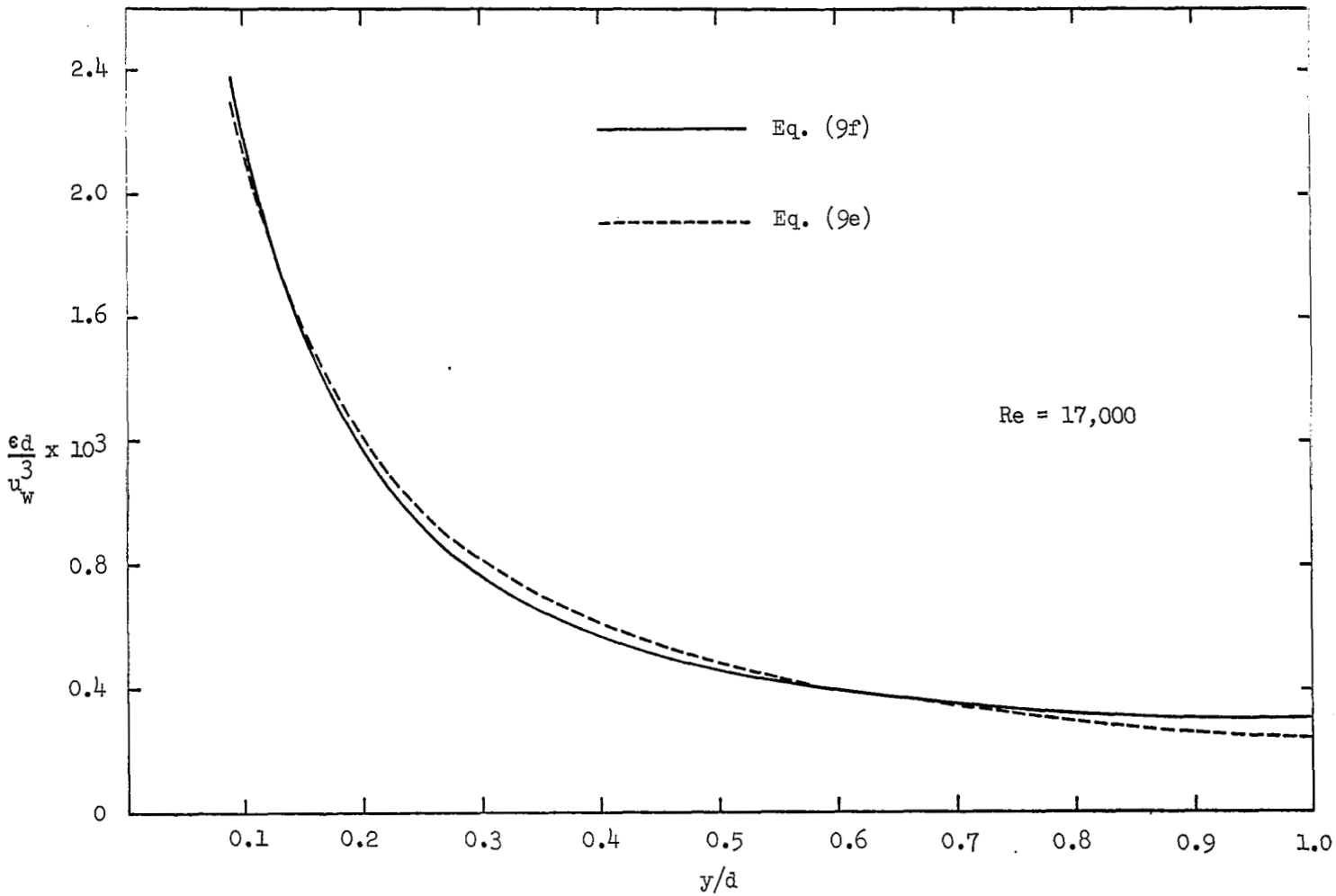

Fig. 12. Turbulence Dissipation Rate, ϵ. Second-order Difference Solution

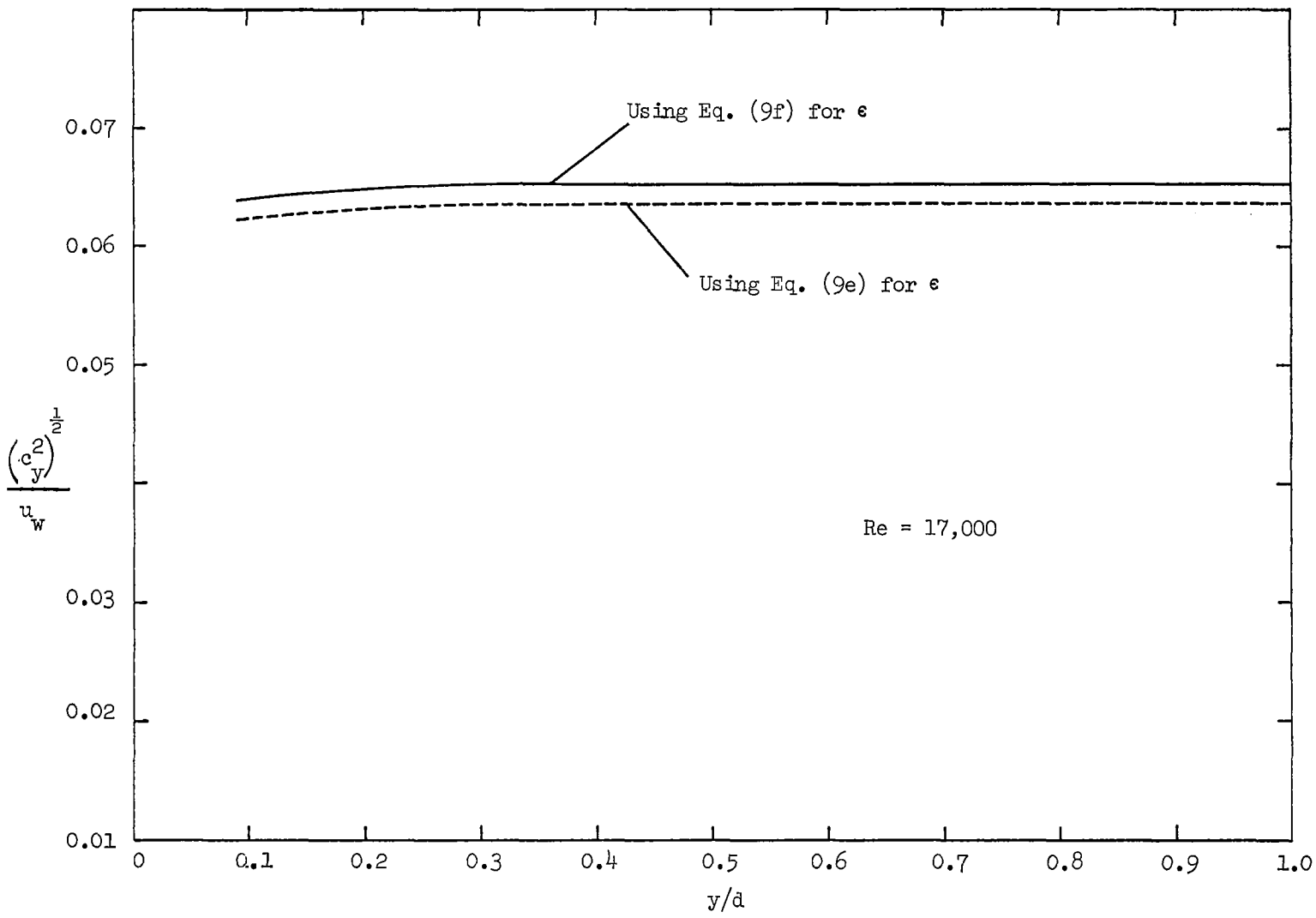

Fig. 13 Root Mean Square of y-component Turbulence Velocity

APPENDIX A

The governing differential equations, Eqs. (9), contain terms which are defined as moments of the distribution functions. Since these moments are obtained as integrals over velocity space, as shown in Eqs. (8), it is convenient to discretize the velocity variable. The set of discrete velocity points selected is denoted by $\{c_\sigma\}$, and a continuous function, say $g(y, c_y)$, is replaced by a set of functions $g_\sigma(y)$, $\sigma = 1, 2 \ldots, S$. This procedure is applied for each of the dependent variables. To evaluate the required moments, numerical quadratures employing appropriate weighting functions may be used. These are of the form

$$\int_{-\infty}^{\infty} \phi(c_y)\ g(y, c_y)\ dc_y \cong \sum_{\sigma=1}^{S} \phi(c_\sigma)\ g_\sigma(y)\ W_\sigma \qquad \text{(A-1)}$$

where ϕ is a function of c_y, and W_σ are the weights in the quadrature.

The specific values for the discrete ordinates, c_σ, depend upon the quadrature selected. In the present study an eleven-point closed-type Newton-Cotes quadrature is employed for integration. This quadrature requires equally spaced points in the interval of integration. To reduce the computing time, the interval of integration is divided into many sub-intervals and appropriate spacings are chosen in each sub-interval.

After some numerical experimentation, a total of 440 discrete velocity points were utilized to insure sufficient accuracy in the integrations.

When discrete ordinates are employed, the governing equation (9a), then becomes a system of differential equations of the form

$$c_\sigma \frac{dg_\sigma}{dy} = \frac{1}{\tau}\left(G_\sigma - g_\sigma\right) + \frac{\epsilon}{3U^2}\left\{g_\sigma + c_\sigma \left(\frac{\partial g}{\partial c_y}\right)_\sigma\right\} \qquad \text{(A-2)}$$

where $\sigma = 1, 2, \ldots, S$. In this system, g_σ is a function of y only, and it represents the function $g(y, c_y)$ evaluated at the discrete velocity point $c_y = c_\sigma$. In the numerical procedure used to solve the set of equations (A-2), the term $\left(\frac{\partial g}{\partial y}\right)_\sigma$ is replaced by a finite difference approximation as described in Appendix B. Thus, the governing partial differential equation, Eq. (9a) is approximated by a set of ordinary differential equations of the form shown in Eq. (A-2). A similar set of equations is obtained for each of the reduced distribution functions. These sets are then solved for the various discretized functions, and the results are used in the numerical quadratures representing integrations over velocity space (Eq. (A-1)).

APPENDIX B

The non-dimensionalized governing equations for the reduced distribution functions are

$$c_y \frac{\partial g}{\partial y} = \frac{1}{\tau}\left(G - g\right) + \frac{\epsilon}{3U^2}\left(g + c_y \frac{\partial g}{\partial c_y}\right) \tag{B-1}$$

$$c_y \frac{\partial j}{\partial y} = \frac{1}{\tau}\left(J - j\right) + \left(\frac{1}{Re_*}\frac{d^2u}{dy^2} - P_k - c_y \frac{du}{dy}\right) g \tag{B-2}$$

$$+ \frac{\epsilon}{3U^2} c_y \frac{\partial j}{\partial c_y}$$

$$c_y \frac{\partial h}{\partial y} = \frac{1}{\tau}\left(H - h\right) + 2\left(\frac{1}{Re_*}\frac{d^2u}{dy^2} - P_k - c_y \frac{du}{dy}\right) j \tag{B-3}$$

$$+ \frac{\epsilon}{3U^2}\left(-h + c_y \frac{\partial h}{\partial c_y}\right)$$

and

$$v_y \frac{\partial j_v}{\partial y} = \frac{1}{\tau}\left(J_v - j_v\right) + \left(\frac{1}{Re_*}\frac{d^2u}{dy^2} - P_k\right) g \tag{B-4}$$

$$+ \frac{\epsilon}{3U^2}\left(u\, g + v_y \frac{\partial j_v}{\partial v_y}\right)$$

Using the second-order finite difference schemes outlined in the section NUMERICAL APPROACH, the Equations (B-1) - (B-4) can be approximated for each node (i,σ) as shown below. The subscript "i" denotes the i^{th} point in the physical space, y_i, and the subscript "σ" represents the discrete velocity point c_σ.

Finite-difference equations for "positive stream", $(c_\sigma > 0)$ can be obtained by using backward differences in physical space and forward differences in velocity space. The reduced distribution functions for "positive stream" are denoted by a superscript "+". Thus, Equation (B-1) can be written, for $c_\sigma > 0$, as

$$\frac{c_\sigma}{2(\Delta y)}\left(3\, g^+_{i,\sigma} - 4\, g^+_{i-1,\sigma} + g^+_{i-2,\sigma}\right) = \frac{1}{\tau}\left(G^+_{i,\sigma} - g^+_{i,\sigma}\right)$$

$$+ \frac{\epsilon_i}{3U^2}\, g^+_{i,\sigma} + \frac{\epsilon_i c_\sigma}{3U_i^2}\left(D_1^+ g^+_{i,\sigma} + D_2^+ g^+_{i,\sigma+1} + D_3^+ g^+_{i,\sigma+2}\right)$$

where

$$D_1^+ = \frac{(2\, c_\sigma - c_{\sigma+1} - c_{\sigma+2})}{(c_\sigma - c_{\sigma+1})(c_\sigma - c_{\sigma+2})}$$

$$D_2^+ = \frac{(c_\sigma - c_{\sigma+2})}{(c_{\sigma+1} - c_\sigma)(c_{\sigma+1} - c_{\sigma+2})}$$

and

$$D_3^+ = \frac{(c_\sigma - c_{\sigma+1})}{(c_{\sigma+2} - c_\sigma)(c_{\sigma+2} - c_{\sigma+1})}$$

Solving for $g^+_{i,\sigma}$, one gets

$$g^+_{i,\sigma} = \left\{ \frac{G^+_{i,\sigma}}{\tau} + \left(\frac{c_\sigma}{\Delta y}\right)\left(2\, g^+_{i-1,\sigma} - \frac{1}{2}\, g^+_{i-2,\sigma}\right) \right. \tag{B-5}$$

$$\left. + \frac{\epsilon_i c_\sigma}{3U_i^2}\left(D_2^+ g^+_{i,\sigma+1} + D_3^+ g^+_{i,\sigma+2}\right)\right\}$$

$$\Big/ \left\{ \frac{3}{2}\,\frac{c_\sigma}{\Delta y} + \frac{1}{\tau} - \frac{\epsilon_i}{3U_i^2} - \frac{\epsilon_i}{3U_i^2}\, c_\sigma\, D_1^+ \right\}$$

Similar expressions for positive stream can be derived for the other reduced distribution functions.

Finite-difference equations for "negative stream", ($c_\sigma < 0$) could be derived by using forward differences in physical and backward differences in velocity space. Equation (B-1) can then be written for "negative stream", $c_\sigma < 0$) indicated by a superscript "-", as

$$\frac{c_\sigma}{2(\Delta\hat{y})}\left(4\,\bar{g}_{i+1,\sigma} - \bar{g}_{i+2,\sigma} - 3\bar{g}_{i,\sigma}\right) = \frac{1}{\hat{\tau}}\left(G_{i,\sigma} - \bar{g}_{i,\sigma}\right)$$

$$+ \frac{\epsilon_i}{3U_i^2}\,\bar{g}_{i,\sigma} + \frac{\epsilon_i}{3U_i^2}\,c_\sigma\left(\bar{D}_1\,\bar{g}_{i,\sigma-2} + \bar{D}_2\,\bar{g}_{i,\sigma-1} + \bar{D}_3\,\bar{g}_{i,\sigma}\right)$$

where

$$\bar{D}_1 = \frac{(c_\sigma - c_{\sigma-1})}{(c_{\sigma-2} - c_{\sigma-1})(c_{\sigma-2} - c_\sigma)}$$

$$\bar{D}_2 = \frac{(c_\sigma - c_{\sigma-2})}{(\hat{c}_{\sigma-1} - c_{\sigma-2})(c_{\sigma-1} - c_\sigma)}$$

and

$$\bar{D}_3 = \frac{(2c_\sigma - c_{\sigma-1} - c_{\sigma-2})}{(c_\sigma - c_{\sigma-2})(c_\sigma - c_{\sigma-1})}$$

Solving for $\bar{g}_{i,\sigma}$, one gets

$$\bar{g}_{i,\sigma} = \left\{ \frac{\bar{G}_{i,\sigma}}{\hat{\tau}} + \frac{c_\sigma}{(\Delta\hat{y})}\left(\frac{1}{2}\,\bar{g}_{i+2,\sigma} - 2\,\bar{g}_{i+1,\sigma}\right)\right. \tag{B-6}$$

$$\left. + \frac{\epsilon_i}{3U_i^2}\,c_\sigma\left(\bar{D}_1\,\bar{g}_{i,\sigma-2} + \bar{D}_2\,\bar{g}_{i,\sigma-1}\right)\right\}$$

$$\Big/\left\{\frac{1}{\hat{\tau}_i} - \frac{3}{2}\frac{c_\sigma}{(\Delta y)} - \frac{\epsilon_\sigma}{3U_i^2} - \frac{\epsilon_i}{3U_i^2}\,c_\sigma\,\bar{D}_3\right\}$$

Similar expressions for negative stream can be derived for the other reduced distribution functions.